IMPROVEMENTS IN GPS TROPOSPHERIC DELAY ESTIMATION WITH NUMERICAL WEATHER PREDICTION

KAREN COVE

May 2005

TECHNICAL REPORT
NO. 230

IMPROVEMENTS IN GPS TROPOSPHERIC DELAY ESTIMATION WITH NUMERICAL WEATHER PREDICTION

Karen Cove

Department of Geodesy and Geomatics Engineering
University of New Brunswick
P.O. Box 4400
Fredericton, N.B.
Canada
E3B 5A3

May 2005

PREFACE

This technical report is a reproduction of a thesis submitted in partial fulfillment of the requirements for the degree of Master of Science in Engineering in the Department of Geodesy and Geomatics Engineering, May 2005. The research was supervised by Dr. Marcelo Santos, and funding was provided by the Natural Sciences and Engineering Research Council of Canada and by the University of New Brunswick.

As with any copyrighted material, permission to reprint or quote extensively from this report must be received from the author. The citation to this work should appear as follows:

Cove, K. (2005). *Improvements in GPS Tropospheric Delay Estimation with Numerical Weather Prediction*. M.Sc.E. thesis, Department of Geodesy and Geomatics Engineering Technical Report No. 230, University of New Brunswick, Fredericton, New Brunswick, Canada, 98 pp.

ABSTRACT

Long baseline, carrier-phase differential GPS positioning in a coastal environment poses unique challenges. It is well known that differential GPS positioning results degrade as baseline length increases due to several sources of error, including the error introduced by differential troposphere. The effect of the troposphere on GPS has been extensively discussed by numerous researchers, either by comparing the resolution of global prediction models or by assessing the tropospheric delay directly on GPS measurements and results.

The goal of this thesis is to examine methods for improving tropospheric delay estimation by using meteorological data. This includes the use of surface meteorological parameters in global prediction models and Numerical Weather Prediction model data in the estimation of the delay. For the tests presented in this thesis, the Saastamoinen global prediction model is used and NWP data are accessed from the Canadian Meteorological Centre's regional model.

Results are presented in the measurement and position domains. In the measurement domain, tropospheric delays modelled from the NWP model and global prediction model are compared with those from the IGS final zenith tropospheric delay product. In the position domain, the estimated delays are applied to kinematic GPS data sets and are evaluated based on short/ long baseline comparisons.

The test results show a significant improvement in the measurement domain with the use of NWP model data in the estimation of zenith tropospheric delay. This improvement does not appear to have positive effect on the position results.

ACKNOWLEDGEMENTS

I would like to express my gratitude to Marcelo Santos, David Wells, and Sunil Bisnath for their support over my graduate studies. The guidance and opportunities you have provided have been invaluable to me.

I would also like to thank and acknowledge Anna Jensen, Technical University of Denmark, and Seth Gutman, Forecast Systems Laboratory, for providing me with access to their NWP related code and Ben Remondi for the use of DynaPos for all my research endeavors and for his personal guidance, help and expertise in the area of GPS data processing.

Acknowledgement is extended to everyone involved in the Princess of Acadia GPS Project including: the Department of Marine Sciences at the University of Southern Mississippi, the Canadian Meteorological Centre for providing the NWP data, the Geodetic Survey of Canada for providing GPS data from the CACS network, the XYZ's of GPS for the use of DynaPos GPS processing software, the National Oceanic and Atmospheric Administration, Canadian Hydrographic Service and University of Dalhousie for installing and maintaining the tide gauges, and finally, the Office of Naval Research and NSERC for funding the project. Particular thanks is extended to the Canadian Coast Guard in Saint John, the staff at Digby Regional High School, and Marine Atlantic and the crew of the Princess of Acadia ferry for generously donating both space for the GPS installations, and effort in helping us make the project a reality

A personal thanks is extended to my husband Andrew, my parents Maureen and David Cove, and my parents in-law Barbara and Peter Morrison for their continuous support and encouragement. Cheers to my office mates, Azadeh, Rodrigo, Huaining, and Felipe, and all my friends and colleagues in GGE.

TABLE OF CONTENTS

LIST OF TABLES

LIST OF FIGURES

LIST OF MAJOR SYMBOLS

Symbol	Designation	Units
d_{trop}	total tropospheric delay	m
d_{ion}	total ionospheric delay	m
e	partial pressure of water vapour	mbars
g	normal gravity	m s^{-2}
h	orthometric height	m
H	geometric height	m
N	total refractivity	N-units
P_d	partial pressure of dry air	mbars
ϕ	latitude	rad
ρ	mass density	kg m^{-3}
P	total pressure	mbars
q	specific humidity	kg kg^{-1}
R_d	mean specific gas constant for dry air	J kg^{-1} K^{-1}
R_w	mean specific gas constant for water vapour	J kg^{-1} K^{-1}
T	absolute temperature	K
U	relative humidity	%
Z_w	compressibility factor for water vapour	unitless
Z_h	compressibility factor for dry air	unitless

1 INTRODUCTION

Current and future modernization of the Global Positioning System (GPS) will result in the troposphere comprising an increasing proportion of the error budget in GPS positioning. This thesis examines the potential use of Numerical Weather Prediction (NWP) in the role of reducing the effect of errors due to the troposphere.

1.1 Motivation

The largest sources of error in differential carrier-phase GPS positioning are clock errors and the propagation of the GPS signal as it passes through the earth's atmosphere. Clock errors can be effectively eliminated with double differencing. Errors associated with the atmosphere are not as easily dealt with. Atmospheric errors are also spatially correlated; therefore, with baselines of tens to hundreds of kilometres, these errors can have a significant effect on position accuracy.

Position accuracies at the centimetre level may improve the feasibility and expand the use of GPS positioning in applications such as vertical control in the measurement and modeling of offshore tidal and other water level variations, offshore determinations of the geoid-ellipsoid separation, hydrographic and land based surveying and navigation, calibration of satellite sensors, and other activities at sea or on land.

In order to reach centimetre level accuracies for baselines exceeding ten kilometres, errors due to the atmosphere must be reduced. The use of dual frequency GPS data effectively eliminates the first order effects of the ionospheric portion of the delay. The tropospheric portion of the delay is dealt with mainly through the use of global prediction models and double differencing (Mendes, 1999). It has been proposed that several tactics could improve on the estimation of tropospheric delay and thus, overall position accuracy. Some of these tactics include improving existing global prediction models, the use of measured meteorological parameters in the existing models, estimating residual tropospheric delay, and the use of NWP model data in the estimation of the delay (Cove and Santos, 2004; Wells *et al.*, 2004).

This thesis is an investigation into the use of NWP model data for the estimation of tropospheric delay of the GPS signal as compared to using a global prediction model. Methods for extracting and using NWP model data for the estimation of tropospheric delay has been introduced by Vedel *et al*. (2001) and Gutman *et al*. (2003). Research by Jensen (2002c), Pany *et al*. (2001b), Bock and Doerflinger (2001), and Schueler et al. (2000) have shown tropospheric delay estimated with NWP model data may result in higher accuracy solutions for GPS positioning. Tsujii *et al*. (2001) and Jensen (2002c) have shown that the use of NWP model data may also improve kinematic ambiguity resolution.

Recently, there has been interest in broadcasting tropospheric corrections for wide area DGPS services. It has been proposed that the corrections could be generated with NWP model data. Research has been performed to investigate the feasibility and

value of using NWP derived tropospheric error estimation for this purpose (Bisnath *et al*., 2004a; Jupp *et al.,* 2003).

In this thesis, we look at using various strategies for improving the estimation of tropospheric delay with the goal of improving solutions for long baseline positioning. The results of using NWP model data to estimate tropospheric delay and its effect on the position solution will be presented.

1.2 Research Objectives

With the planned modernization of the GPS infrastructure and signals, much future research into improving positioning for long baseline application will be focused on the troposphere. It has been shown that the use of 3-dimensional NWP model data is useful in modeling the effects of the troposphere on the GPS signal.

The main objective of this research is to introduce the reader to the potential use of NWP in the estimation of tropospheric delay for GPS positioning. This goal is divided into three distinct parts: how NWP model data is used in the estimation of the delay, the results of using NWP model data in the measurement domain, and the results of using the NWP generated delays in the position domain.

1.3 Thesis Outline

Chapter 2 The first part of the thesis is intended to provide the reader with a general overview of differential carrier-phase GPS positioning. The chapter will emphasize issues relevant to the positioning test performed in Chapter 5, in particular, the role of inter-frequency linear combinations in obtaining an optimal positioning result.

Chapter 3 A description of the neutral atmosphere and an explanation of the basic theory of the effect of the neutral atmosphere on the GPS signal, referred to as tropospheric delay, and how the effect is modeled for GPS positioning. The Saastamoinen global prediction model and the Niell mapping function are introduced.

Chapter 4 An introduction to Numerical Weather Prediction and its potential role in GPS positioning. The NWP model used in the tests presented in Chapter 5 is described in detail along with the equations required to calculate tropospheric delay from the model.

Chapter 5 A presentation of the data and results used to test the use of NWP model data for GPS positioning. The test data is part of a research project with the goal of extending the range and improving the accuracy of marine post-processed kinematic GPS positioning. Testing of the use of NWP model data for the estimation of tropospheric delay takes place in the measurement and position domains.

Chapter 6 The final chapter of the thesis offers some concluding remarks and recommendations for future research efforts on the topic.

Appendix A Coordinates of GPS stations in ITRF and NAD83 (CSRS).

Appendix B Description of the process for determining station barometric pressure for use in the estimation of tropospheric delay with NWP model data.

Appendix C The expression for determining normal gravity.

Appendix D Description of the SINEX_TRO format.

Appendix E Detailed graphs of the temperature, relative humidity, and pressure at GPS stations UNB1, CGSJ, DRHS, and BOAT for the test evaluation periods.

Appendix F Daily results for measurement domain tests.

Appendix G Zenith total delays at station CGSJ.

Appendix H Histogram plots of differences in total zenith delay.

2 REVIEW OF CARRIER-PHASE DIFFERENTIAL GPS POSITIONING

Originally designed by the United States Department of Defence for military use, GPS has also become the primary radio positioning navigation system for civilian users. GPS signals are transmitted on carriers at two frequencies, L1 at 1575.42 MHz and L2 at 1227.60 MHz. The carriers are modulated by pseudorandom noise codes, a C/A code and P code, in order to provide GPS receivers with satellite clock readings. On the L1 frequency the C/A code is emitted at 1.023 MHz every millisecond and the P code is emitted at 10.23 MHz every 266.4 days. The L2 frequency only carries a P code. A navigation message containing information about the satellite's orbit parameters and clock corrections is sent every 30 seconds at a frequency of 50 Hz (Misra and Enge, 2001).

The GPS system provides two types of measurements for positioning: code-phase and carrier-phase measurements. Code-phase measurements are instantaneous and provide range measurements from satellite to receiver. The measurement is made by the apparent transit time of the signal between the satellite and receiver. Carrier-phase measurements are made by comparing the received carrier phase to the phase of a sinusoidal signal generated by the receiver clock. This provides a precise measurement of the change in the satellite to receiver range over time and an estimate of the instantaneous rate (Misra and Enge, 2001). For precise positioning applications, including those included in this thesis, the carrier-phase measurement is used.

The following sections are focused on introducing the carrier-phase observation equation, identifying sources of error relevant to long baseline positioning, i.e., tens to hundreds of kilometers, and identifying mitigation strategies for dealing with them including double differencing and the use of inter-frequency linear combinations. Comprehensive sources on the subject of carrier-phase positioning can be found, for example, in Misra and Enge (2001) and Wells *et al.* (1986).

2.1 Carrier Phase Observable Equation

GPS positioning at the centimetre and millimetre level require the use of the carrier-phase measurement. The carrier phase observable equation for GPS, in units of length, is expressed (Wells *et al.*, 1986) as:

$$\varphi = \rho + d\rho + c \cdot (dt - dT) + \lambda \cdot N - d_{ion} + d_{trop} + d_{mp} + \varepsilon \quad , \tag{2.1}$$

where φ is the carrier-phase observation, ρ is the geometric distance between the satellite and receiver positions, $d\rho$ is the effect of ephemeris errors, c is the speed of light, dt is the satellite clock error, dT is the receiver clock error, λ is the carrier-phase wavelength, N is the integer ambiguity, d_{ion} is the ionospheric delay, d_{trop} is the tropospheric delay, d_{mp} is the multipath effect, and ε is the observation noise. The basic observable is the difference between the Doppler-shifted carrier signal transmitted by the satellite and that

of the receiver's internal oscillator. The signal is made up of some finite number of full cycles and a left over fraction of a cycle. The inherent problem of measuring carrier phase is that each cycle is exactly the same. This means that the actual integer number of cycles in the signal between the receiver and satellite is unknown or ambiguous. In order to estimate the integer number, the receiver measures the fractional phase; a processing technique called ambiguity resolution to determine the integer value (Misra and Enge, 2001).

2.2 Sources of Error

Several sources of error limit position accuracy in GPS positioning. Most errors can be substantially reduced or effectively eliminated through the use of specialized equipment, and/or processing techniques. In the case of differential positioning errors and biases due to orbit errors, clocks, and the atmosphere are substantially reduced through double differencing (see Section 2.3). Further improvements to biases due to orbit errors can be achieved through post-processing with precise ephemeredes. Multipath can be minimized with the use of multipath resistant equipment such as choke-ring antennas (Wells *et al*., 1986).

The errors due to the atmosphere are large in magnitude and must be substantially reduced in order to achieve precise positioning results. The ionosphere is a dispersive medium for GPS frequencies so the signal delay due to passing through this

layer of the atmosphere can be almost completely eliminated with dual-frequency processing in most cases. The troposphere is a non-dispersive medium at these frequencies so the error must be reduced with the use of global prediction models (Wells *et al*., 1986). This method, however, is not always effective and differential troposphere remains as the most significant source of error for long baseline positioning. A reduction in the magnitude of this error may be possible through improved modelling of the neutral atmosphere. A more detailed discussion of the effect of the troposphere on GPS signals can be found in Chapter 3.

2.3 Double Differencing

Differential positioning is the determination of a position in latitude, longitude, and height relative to a known position. This requires the use of two GPS receivers taking measurements during a common time interval. Simultaneous observations allow for the observation equations to be differenced. This can reduce the effect of some common biases and errors such as: satellite orbit biases, clock biases, and atmospheric delays. The amount the orbit and atmospheric biases are reduced is largely dependent on the baseline distance that separates the two receivers as the troposphere and ionosphere can vary greatly over large distances (Misra and Enge, 2001).

In relative GPS positioning a series of differenced equations can result in an improved position solution by diminishing or eliminating many of the sources of error

and bias that appear in the GPS observable equation. A between receiver single difference is the difference between the phase equation for a receiver at one location and a satellite and the corresponding phase equation for a second receiver at another location and the same satellite. The single difference equation is expressed (Wells *et al*., 1986) as:

$$\Delta\varphi = \Delta\rho + \Delta d\rho + c \cdot \Delta dT + \lambda \cdot \Delta N - \Delta d_{iom} + \Delta d_{trop} + \Delta d_{mp} + \Delta\varepsilon \ , \qquad (2.2)$$

where Δ represents the difference between two. This effectively eliminates the satellite clock error, dt, and reduces the error associated with orbit and some of the atmospheric delay.

A double difference is the subtraction of one single differenced phase equation from another at the same epoch and can be expressed (Wells *et al*., 1986) as:

$$\nabla\Delta\varphi = \nabla\Delta\rho + \lambda \cdot \nabla\Delta N - \nabla\Delta d_{ion} + \nabla\Delta d_{trop} + \nabla\Delta d_{mp} + \nabla\Delta\varepsilon \ , \qquad (2.3)$$

where $\nabla\Delta$ represents the operator for double differencing. The receiver clock error, dT, is effectively eliminated. The biases and errors associated with the orbit and atmosphere will each be reduced from the original values but the amount of the reduction is baseline distance dependent. All sources of error within the equation must be effectively eliminated, reduced, modelled, or solved before the integer ambiguity can be resolved.

2.4 Inter-frequency Linear Combinations

Inter-frequency data combinations are employed in processing in order to obtain an optimum position solution. These are designed to minimize the biases that affect longer baseline positioning and/ or to facilitate the resolution of integer ambiguity.

The general form of all inter-frequency linear combinations (Misra and Enge, 2001) is expressed as:

$$\varphi_L = n\varphi_{L1} + m\varphi_{L2} \ , \tag{2.4}$$

where n and m are arbitrary numbers. The three most widely used combinations are the narrow-lane (φ_{LN}), wide-lane (φ_{LW}), and ionospheric delay-free (φ_{LIF}) combinations obtained by assigning the appropriate value to n and m, as:

$$\varphi_{LN} = \varphi_{L1} + \varphi_{L2} \ , \tag{2.5}$$

$$\varphi_{LW} = \varphi_{L1} - \varphi_{L2} \ , \tag{2.6}$$

$$\varphi_{LIF} = \varphi_{L1} - \left(\frac{f_{L1}}{f_{L2}}\right)\varphi_{L2} \ , \tag{2.7}$$

where n =1 and m = 1 in the narrow-lane combination, n =1 and m = -1 in the wide-lane combination, and n = 1 and $m = -\left(\frac{f_{L1}}{f_{L2}}\right)$ in the ionospheric delay-free combination (Misra and Enge, 2001).

The narrow-lane combination is used primarily to achieve high accuracy results in short baseline applications. This is possible due to the short wavelength, 10.7 centimetres, and consequently low noise generated by the combination. The short wavelength, however, does result in some difficulties in ambiguity resolution due to the narrow window the wavelength provides.

In medium and long baseline positioning, the wide-lane and ionospheric delay-free combinations are used to improve position accuracy. In this case, medium range is defined as anything between 10 to 100 kilometres and long range as anything between 100 kilometres and thousands of kilometres. The wide-lane combination aids in the resolution of the integer ambiguity by increasing the wavelength of carrier. This increases the opportunity of resolving the integer ambiguity, but with the trade off of a higher noise level. For the carrier-phase based positions to achieve millimetre accuracies the integer ambiguity must be solved using some kind of ambiguity resolution technique, otherwise only centimetre and decimetre level accuracies will be reached (Han, 1997). Typically, the ability to resolve the integer ambiguity is only valid for baselines less than 10 to 15 kilometres. The chances of incorrectly solving the integer ambiguity would be too great beyond that range (Santos *et al.*, 2000). The ionospheric delay-free combination is appropriate for longer baseline cases as it minimizes the effect of the

ionosphere, often the most significant source of error as baseline length increases, with the elimination of the first order ionospheric effects. In times of high ionospheric activity, remaining higher order ionospheric effects may result in significant residual error in long baseline positioning (Jensen, 2002c). The downfall of this combination is that the integer nature of the ambiguities is destroyed making it significantly noisier than the pseudorange measurements at L1 and L2 (Misra and Enge, 2001).

3 MODELLING THE TROPOSPHERE

The GPS signals experience a change in speed and direction as they pass through the atmosphere from the satellite to the receiver. Of the approximate 20000 to 26000 kilometre journey the signal travels, only the last 5percent of the path will be through the earth's atmosphere. In the remaining 95percent the signal can be considered to travel through a vacuum with a constant speed. The portion of the earth's atmosphere affecting the GPS signal is made up of the ionosphere and the neutral atmosphere. As discussed in Chapter 2, the refraction affecting the signal as it passes through the ionosphere can be effectively eliminated during processing with the use of dual frequency signals (Wells *et al*., 1986). The effect of the neutral atmosphere on GPS signals cannot be completely removed during processing, except for short baselines, and remains a significant source of error for medium and long baseline positioning.

This chapter offers a description of the neutral atmosphere and how the delay due to the neutral atmosphere, referred to as tropospheric delay, can be modelled. This chapter primarily presents material relevant to the tests presented in Chapter 5; a comprehensive discussion on modelling the neutral atmosphere can be found in Mendes (1999).

3.1 The Neutral Atmosphere

The neutral atmosphere refers to the non-ionized portion of the atmosphere made up of the lower part of the stratosphere and the troposphere. The troposphere makes up the lower portion of the neutral atmosphere, extending from the earth's surface up to an altitude of approximately 16 kilometres at the equator and 8 kilometres at the poles. The actual upper boundary of the troposphere, or the tropopause, is dependent on factors of latitude, season and changes in surface pressure. The stratosphere extends upwards from the tropopause to approximately 50 kilometres in altitude. Even though gradually decreasing quantities of dry gases can extend several hundred kilometres in altitude, all of the water vapour and the bulk of the dry gases are found in the troposphere. The density of the dry gases and water vapour in the atmosphere determines the extent the signal is refracted or delayed. Accordingly, the refraction of the GPS signal as it passes through the entire neutral atmosphere is referred to as tropospheric delay (Misra and Enge, 2001; Barry and Chorley, 1998).

The speed of propagation of GPS signals through the neutral atmosphere is lower than in free space. Consequently, the tropospheric delay causes the distance travelled by the signal to be longer than the actual geometric distance between satellite and receiver. Since the medium is non-dispersive, the measurements at all GPS signal frequencies for code and carrier experience the same delay (Misra and Enge, 2001).

The effect of the tropospheric delay on the GPS signal is modelled with the use of the equation for refractivity in the form of a global prediction model. These models

use surface meteorological parameters, such as temperature, pressure and relative humidity, and station specific information, such as height and latitude of the receiver, to estimate the magnitude of the tropospheric delay. Researchers have found the use of 3 dimensional meteorological data, such as provided by NWP models, to be a more effective method for estimating tropospheric delay than with surface meteorological data in global prediction models (Vedel, *et al*., 2001; Jensen, 2002c; Gutman *et al*., 2003).

3.2 Modelling Zenith Tropospheric Delay

Water vapour and dry gases found in the neutral atmosphere affect the propagation of the GPS signal. Typically, the hydrostatic component of the delay in the zenith direction is in the range of 2.3-2.6 metres and represents about 90 percent of the total delay. As found by Mendes (1999), the hydrostatic component of the delay can be modeled to sub-millimetre accuracy with the use of prediction models such as Saastamoinen (1973). The highly variable non-hydrostatic delay, however, can only be estimated with predictive models to an accuracy of a few centimetres in the zenith direction. Further error is introduced when the zenith delay is mapped to the elevation angle of the satellite with the use of a mapping function such as, e.g., Niell (1996).

The delay of the GPS signal as it passes through the neutral atmosphere can be expressed as the sum of the hydrostatic (N_h) or 'dry' and non-hydrostatic (N_w) or 'wet' refractivities, due to the effects of dry gases and water vapour, respectively.

$$N = N_h + N_w \quad , \tag{3.1}$$

The zenith total delay (*ztd*) of the signal is determined by integrating the refractivity along the signal path (*dl*) as:

$$ztd = 10^{-6} \int N_h dl + \int N_w dl \quad , \tag{3.2}$$

where refractivity, N, is expressed as (Thayer, 1974):

$$N = k_1 \left(\frac{P_d}{T} \right) Z_h^{-1} + \left(k_2 \frac{e}{T} + k_3 \frac{e}{T^2} \right) Z_w^{-1} \quad , \tag{3.3}$$

where k_1, k_2, and k_3 are refractivity constants in Kelvin millibars^{-1} (for k_1 and k_2) and Kelvin^2 millibars^{-1} (for k_3), P_d is the partial pressure of dry gases in millibars, e is the partial pressure of water vapour in millibars, T is the temperature in Kelvin (K), Z_h is the compressibility factor for dry air and Z_w is the compressibility factor for water vapour.

The tropospheric delay from GPS signals can be estimated in several ways: by determining the zenith tropospheric delay by applying a global prediction model, by ray tracing through the atmosphere on a path that approximates that of the signal, or by some other method such as integrating through a NWP model. Although, ray tracing provides a better estimate of the delay (Mendes, 1999; Jensen, 2002b) only the global

prediction model and NWP methods will be investigated further. This can be justified as the improvements found by ray tracing are significant only at lower elevation angles, such below 10 degrees; a satellite elevation angle mask of 10 degrees will be used in all tests presented in Chapter 5 of this thesis. For a comprehensive review of mapping functions and ray tracing see Mendes (1999) and for comparisons of results for mapping functions and ray tracing see Jensen (2002b), Vedel *et al*. (2001), or Pany *et al*. (2001a).

Alternatively, water vapour in the atmosphere can be measured directly with a water vapour radiometer or derived from a network of GPS stations, such as SuomiNet. SuomiNet is a global network of GPS stations equipped with meterological sensors to generate near real-time estimates of precipitable water vapor in the atmosphere. Direct and GPS derived water vapour measurements are used to improve moisture observations to support weather forecasting, climate monitoring, and research. For more information on SuomiNet or similar programs such as the GPS-Met Observing Systems Branch in the Forecast System Laboratory (FSL) at the National Oceanic and Atmospheric Administration (NOAA) see http://www.suominet.ucar.edu/ and http://www.gpsmet.noaa.gov/jsp/index.jsp, respectively.

3.2.1 Global Prediction Models

A variety of global tropospheric delay prediction models exist; each of these varies in how water vapour and temperature changes with altitude (Misra and Enge,

2001). One of the more common and best performing of the prediction models is Saastamoinen (Mendes, 1999).

The Saastamoinen model (1973) is based on refractivity derived using the gas laws. The hydrostatic (*zhd*) and wet (*zwd*) components of the delay in the zenith direction are expressed as:

$$zhd = 0.002277\left(1 + 0.0026\cos 2\phi + 0.00028h\right)P \ , \tag{3.4}$$

$$zwd = 0.002277\left(\frac{1255}{T} + 0.05\right)e \ , \tag{3.5}$$

where ϕ is the latitude of the receiver in radians, h is the orthometric height of the receiver in kilometres, P is atmospheric pressure in millibars, T is temperature in Kelvin, and e is partial pressure of water vapour in millibars.

Mendes (1999) finds that the total error in the zenith direction for the Saastamoinen model is on average 0.2 millimetres for the dry component and about 30 millimetres for the wet component of the prediction model. These total error statistics are based on comparisons to ray traced values from 50 radiosonde stations worldwide. The Saastamoinen global prediction model is used in all tests presented in Chapter 5.

3.2.2 Mapping Functions

The zenith total delay experienced by the GPS signal can be mapped to the elevation angle between the satellite and receiver with a mapping function. Depending on the mapping function used, the wet and dry components can be incorporated together or treated separately.

In its simplest form, a mapping function for both wet and dry components can be expressed as:

$$m(E) = \frac{1}{\sin E} \ , \tag{3.6}$$

where E is the elevation angle between the satellite and receiver. This model, however, assumes a flat earth and does not provide a good approximation for low elevations. More complex models are based on a truncated form of continued fraction with empirically determined constants and variables related to the latitude, height, time and surface meteorological parameters at the receiver location (Misra and Enge, 2001).

One of the best performing mapping function is the one attributed to Niell (1996) referred to as the Neill (New) mapping Function (NMF). This model is based on temporal fluctuations of the bulk of the atmosphere and requires receiver station height and latitude parameters, but does not require specific meteorological data (Mendes, 1999). The NMF is recommended by the International Earth Rotation Service

(McCarthy and Petit, 2003) for use in the absence of accurate meteorological data at the receiver site. See Mendes (1999) for the complete expression of the NMF.

The path length of the GPS signal increases as elevation angle decreases. Correspondingly, the delay experienced by the signal increases with elevation angle making the residual error in the estimation of the delay more significant at low elevation angles. As a typical example, a 5 centimetre residual error in tropospheric delay at zenith would become a 50 centimetre error at an elevation angle of 5 degrees (Misra and Enge, 2001). The magnitude of the delay at low elevation angles demonstrates the need to employ an effective mapping function.

4 NUMERICAL WEATHER PREDICTION FOR GPS POSITIONING

Researchers have found the use of NWP model data to be a way of estimating tropospheric delay with a higher accuracy than global prediction models. It has been found that the use of regional NWP model in the estimation of zenith troposheric delay gives accuracies in the range of 10 to 20 millimetres as compared to radiosonde data and GPS derived delays (Shueller *et al*., 2000; Bock and Doerflinger, 2000; Pany *et al*., 2001a; Vedel, *et al*., 2001; Jensen, 2002b; Bisnath *et al*., 2004a; Cove *et al*., 2004).

The following sections will present general information about NWP models, specific information about the NWP model produced by the Canadian Meteorological Centre (CMC), and a review of how the refractivity equation presented in Section 3.2 can be used to determine tropospheric delay through a NWP model.

4.1 Introduction to Numerical Weather Prediction

Numerical Weather Prediction models are a three dimensional representation of the atmosphere structured as a series of pressure levels covering a grid area. Numerical Weather Prediction is based on the principle that if the present state of the atmosphere and the laws that govern the atmosphere are known then the evolution of the atmosphere can be forecasted into the future. This procedure is limited by several factors. Firstly,

errors in the assumed state of the present atmosphere will propagate and amplify in the forecast. Secondly, errors exist in how the theoretical laws that govern the behaviour of the atmosphere are modelled and applied. Particularly relevant to the estimation of tropospheric delay are errors in the modelling of water vapour (Pany *et al*, 2001a). Finally, the model is limited by grid resolution. A larger scale model, i.e., smaller grids size, will better represent smaller events and phenomenon (Hess, 1979; Canadian Meteorological Centre, 2002).

During a process referred to as assimilation, the model is updated periodically with quality controlled meteorological data collected globally from a variety of sources including, but not limited to: meteorological observations at the earth's surface and in the air column by sensors such as radiosondes, meteorological stations mounted on platforms such as aircraft, vessels, and buoys, and networks of ground based meteorological and GPS stations. An interpolation scheme must be used to integrate the irregularly spaced observed data into the gridded area covered by the NWP model (Canadian Meteorological Centre, 2002).

Research in the area of using NWP model data for the estimation of tropospheric delay has been done primarily using NWP models produced in Europe and in the United States. Some work has been undertaken to prove legitimacy and usefulness of this approach but little comprehensive work on the subject has been published thus far. The research presented in Chapter 5 is focused on the use of the Canadian NWP model.

4.2 GEM NWP Regional Model Description

The Global Environmental Multiscale (GEM) is the NWP model produced by the CMC. Global and Regional operational runs of model are produced daily and disseminated to the public via the World Wide Web. The global model covers the entire globe and is used for long-range weather forecasting. The regional model is applicable only for short-range weather forecasting in North America. Only the data accessed from the regional run of the GEM model was used for this research.

The Regional operational model produces an analysis and 48 hour forecast twice daily at 00 Z and 12 Z. Figure 4.1 provides a schematic of the assimilation cycle that each global and regional operational run undergoes in order to produce an analysis and forecast. Each of the Regional model runs begins as a trial field based on the Global model run followed by an analysis "spin-up" cycle where observed data is fed into the model to produce a regional analysis and a 6 hour forecast in a process called assimilation. Upon completion of the 12 hour spin up cycle, the regional operational model run is produced with an analysis for time T and a 48 forecast. The forecast is produced in 1 hour increments but is only made available to the public in 3 hour increments (Canadian Meteorological Centre, 2002; Laroche, 1998; Hogue *et al*., 1998).

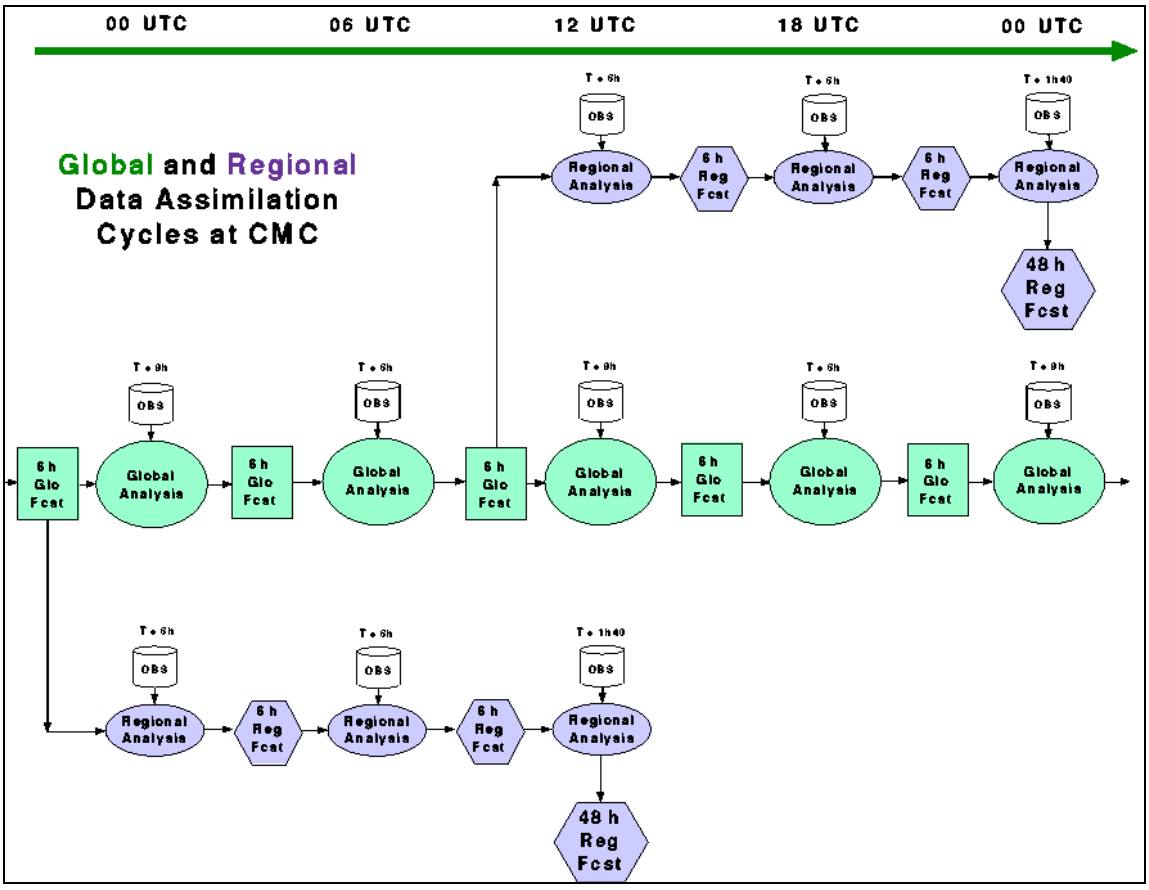

Figure 4.1 Global and Regional data assimilation cycles at the Canadian Meteorological Centre for the GEM model (from Laroche, 1998).

The Regional GEM model is based on a non-uniform grid with a resolution of 15 kilometres, upgraded on 18 May 2004 from a 24 kilometre grid, at the central core. As seen in Figure 4.2, the dataset covers a 501 x 399 Polar-Stereographic grid that covers most of North America and adjacent waters.

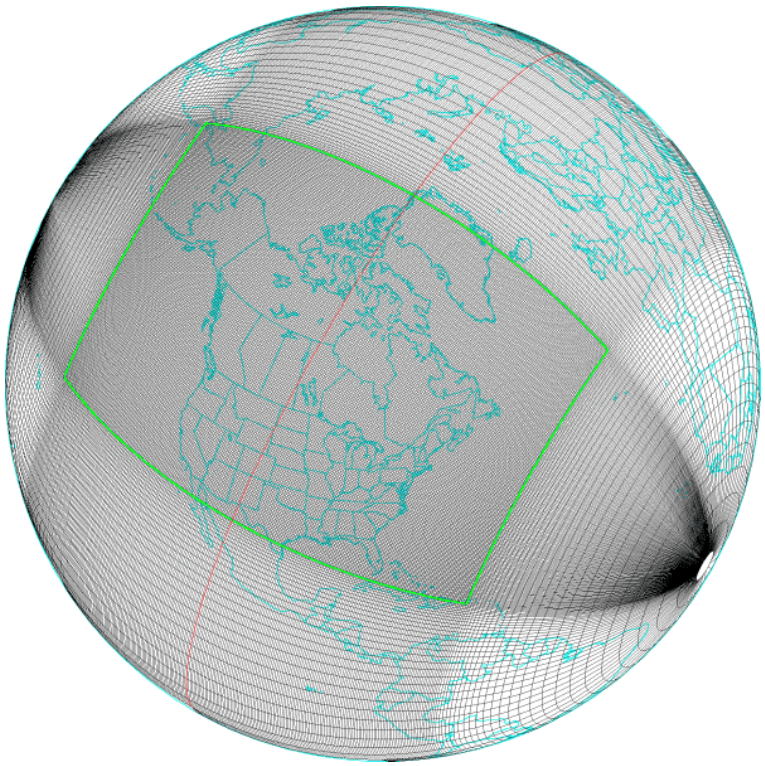

Figure 4.2 Regional grid covering North America and adjacent waters. (From Canadian Meteorological Center, 2002).

The grid is comprised of 28 levels stacked vertically (at pressure levels 50, 100, 150, 175, 200, 225, 250, 275, 300, 350, 400, 450, 500, 550, 600, 650, 700, 750, 800, 850, 875, 900, 925, 950, 970, 985, 1000, and 1015 millibars) extending from an equi-potential representation of the earth's surface to a virtual altitude of 30 kilometres. The regional model contains 30 meteorological variables including parameters such as wind speed, temperature, and relative humidity (Canadian Meteorological Centre, 2002).

Also produced by the CMC are high-resolution runs of the GEM model with a 10 kilometre grid spacing. This version of the model has a finer resolution grid and

additional vertical layers but, is not yet available to the public and was, therefore, not used in the tests presented in Chapter 5. Further information on the global, regional, or high resolution versions of the GEM model can be accessed on the Environment Canada website at http://www.weatheroffice.ec.gc.ca.

4.3 Modelling Tropospheric Delay with NWP Data

Tropospheric delays can be obtained directly by integrating the refractivity along the path of the GPS signal through the neutral atmosphere to obtain a slant delay or by integrating vertically to obtain a zenith delay. The equation for refractivity, N, given in Equation 3.3, can be expressed in terms of height as:

$$\begin{aligned} ztd &= 10^{-6} \int_{h_{ant}}^{h_{top}} k_1 R_d \rho dh \\ &+ 10^{-6} \int_{h_{ant}}^{h_{top}} \frac{R_d}{\in} \left(k_2 - k_1 \in + \frac{k_3}{T} \right) q \rho dh \end{aligned} , \tag{4.1}$$

where R_d is the gas constant for dry air, ρ is the mass density, $\in$ is the ratio between the gas constant for dry air and the gas constant for water vapour, and q is the specific humidity in kilograms / kilograms.

To express the delay in terms of pressure rather than height one must introduce the hydrostatic equation (Wallace and Hobbs, 1977):

$$\delta p = -\rho g dh \ , \tag{4.2}$$

where g is gravity in metres / second^2. The final expression of total zenith tropospheric delay is given (Vedel *et al.,* 2001; Jensen, 2002a) as:

$$ztd = 10^{-6} \int_{p_{ant}}^{p_{top}} k_1 \frac{R_d}{g} dp + 10^{-6} \int_{p_{ant}}^{p_{top}} \frac{R_d}{\in} \left(k_2 - k_1 \in + \frac{k_3}{T} \right) \frac{q}{g} dp \ , \tag{4.3}$$

The temperature (T), pressure (P) and specific humidity (q) parameters are extracted from the NWP model and a total zenith delay (*ztd*) is calculated at each pressure level. A prediction model is used to estimate the delay for the atmosphere above the top pressure level. The expression of the delay in terms of pressure rather than height is appropriate with use of NWP data since the modelled atmosphere is divided into pressure levels.

5 TESTING NUMERICAL WEATHER PREDICTION FOR GPS POSITIONING

The use of NWP model data in the estimation of tropospheric delay was tested for a network of GPS stations in the Bay of Fundy on the east coast of Canada. The delays obtained from the NWP process were compared to delays produced by the IGS and delays obtained with the use of a global prediction model. Tests were performed in the measurement and position domains.

The test area in the Bay of Fundy provides highly variable weather conditions in a coastal environment with a number of GPS reference stations and meteorological stations in the vicinity. The GPS and meteorological data were collected on a regularly scheduled ferry route between Saint John, New Brunswick, and Digby, Nova Scotia. The data exhibit a great deal of spatial and temporal diversity. GPS and meteorological data were collected near the ferry terminals at each end of the route and on the ferry. Data from other continuously operating reference stations (for example the International GPS Service (IGS) station UNB1) were also collected. The data collection began in October 2003 and was terminated in December 2004.

Results show a significant improvement in the use of NWP model data for the estimation of zenith tropospheric delay in the measurement domain over the Saastamoinen global prediction model. This improvement in the measurement domain however, does not translate into an improvement in the position domain.

5.1 Test Data Description

All test data was collected in the eastern coast of Canada, in and around the Bay of Fundy, in the provinces of New Brunswick and Nova Scotia. This locale was chosen for its representation of a marine environment, availability of a vessel to act as a roving platform, and the distribution of reference station in the area. The data were collected and archived for use in a wide variety of research activities; only a subset of the data collected was used in this thesis.

The GPS stations were established on either side of the Bay of Fundy where a ferry, also equipped as a roving GPS station (BOAT), makes daily crossings across the bay. The two base stations were established near the ferry terminals in St. John (CGSJ) and Digby (DRHS). A total of three other permanent stations already in operation by other organizations were also used. One station is an International GPS Service (IGS) station UNB1 operated by the University of New Brunswick in Fredericton, New Brunswick. The two additional stations are Canadian Active Control System (CACS) stations FRED and HLFX, located in Fredericton and Halifax, Nova Scotia, respectively, operated by the Geodetic Survey Division of Natural Resources Canada (NRCan). Figure 5.1 shows the relative location of all stations including approximate relative distances between the reference stations.

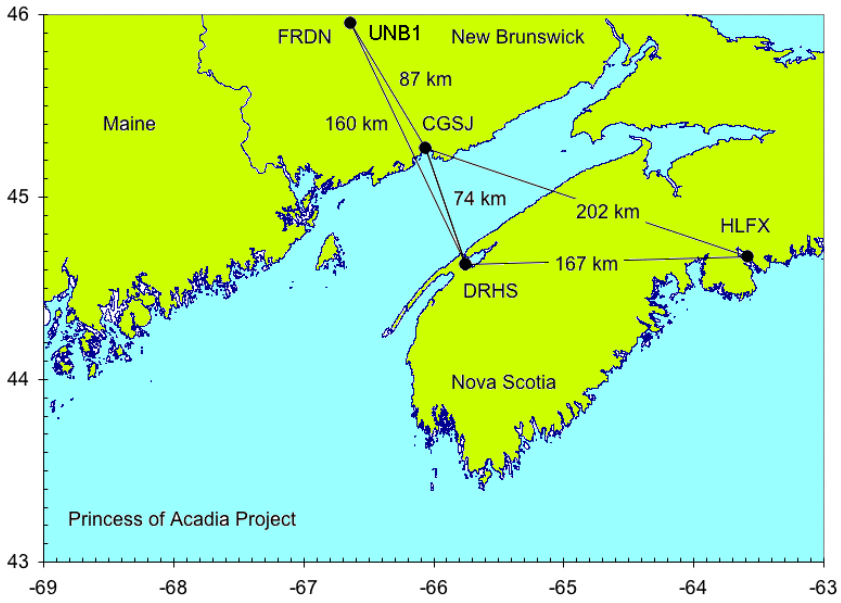

Figure 5.1 Test area in the Bay of Fundy on the East coast of Canada.

The rover receiver was operated on board the ferry *The Princess of Acadia* operated by Bay Ferries Ltd.

Four distinct time periods were chosen to represent weather conditions in the test area. Each period tested consisted of at least four consecutive days with data beginning at hour 0 UTC on the first day and ending on hour 24 UTC on the last. Measurement domain results are based on the entire test period while; position domain results are based on selected time series varying from one hour to three hours during the test periods. The time series selected for the position domain tests represent times when the roving receiver on the ferry was in dock at the ferry terminal in Digby. This provided a 74 kilometre baseline between CGSJ in Saint John and the ferry and a short (less than 5 kilometres) baseline between DRHS in Digby and the ferry docked at the ferry terminal.

The data used for this thesis have been collected as part of a project aimed at the advancement of the science of modelling microwave tropospheric delay over marine areas. The project is funded by the Office of Naval Research (ONR) and is operated by the University of New Brunswick and the University of Southern Mississippi. Additional partners include the Canadian Coast Guard (CCG), the Canadian Meteorological Centre (CMC), Geodetic Survey Division (GSD) at Natural Resources Canada (NRCan), National Oceanic and Atmospheric Administration (NOAA), and the Canadian Hydrographic Service (CHS). Detailed project descriptions and early findings are presented in Cove and Santos (2004b), Bisnath *et al*. (2004b), Santos *et al*. (2004), and Wells *et al*. (2004).

Several sources of scientific data were used in the tests presented in Section 5.2. A brief description of the sources of data including GPS data, surface meteorological data, and NWP data is presented in the following sections.

5.1.1 GPS Data

GPS data from the network of reference stations and the roving platform aboard the Princess of Acadia ferry were collected and archived over a one year period. Data from all station were collected at 1 Hertz, excepting UNB1 with a data rate of 30 seconds. Equipment at CGSJ, DRHS and BOAT stations consisted of Novatel OEM4

GPS receivers with 600 series antennas and Campbell Scientific meteorological stations. The GPS data were stored on an on-site computer.

Equipment at the UNB1 station consists of a JPS LEGACY receiver with a JPSREGANT_DD_E antenna logging at a rate of 30 seconds. Equipment at FRED and HLFX stations consists of AOA BENCHMARK ACT receivers with Dorne Margolin AOAD/M_T antennas. Coordinates for reference stations are given in ITRF and NAD83 (CSRS) in Appendix A.

5.1.2 Surface Meteorological Data

Meteorological data was collected and archived for GPS stations CGSJ, DRHS, and BOAT. These sites were equipped with Campbell Scientific meteorological stations with CR10X data loggers, relative humidity and temperature probe, and a barometric pressure sensor. Detailed specifications, as per the manufacturer under ideal circumstances (Campbell Scientific, 2005), for each probe is presented in Table 5.1.

Table 5.1 Meteorological sensor data for stations CGSJ, DRHS, and BOAT.

Parameter	Manufacturer	Model	Range	Accuracy
Temperature	VAISALA	HMP45C	-39.2 to +60 °C	± 0.2 °C
Relative Humidity	VAISALA	HMP45C	0.8 to 100%	± 1% RH
Barometric Pressure	VAISALA	CS105	600 to 1060 mbar	± 0.5 mbar

Temperature is recorded in degrees Celsius (°C), relative humidity as a percent (%), and barometric pressure in millibars (mbar). The relative humidity and temperature probe, located in a protective radiation shield, was programmed to make a measurement every 15 seconds. The average temperature and relative humidity measurement over a 10 minute period was recorded to the data logger. Barometric pressure was measured and logged once per hour.

All other GPS reference station sites also have meteorological data available. UNB1 station is located in close proximity to SuomiNet station UNB2 in Fredericton. A Paroscientific MET3A instrument measures temperature, relative humidity, and pressure data for SuomiNet station sites. Detailed specifications, as per the manufacturer under ideal circumstances (ParoScientific, Inc., 2004), for meteorological sensors used in the SuomiNet network is presented in Table 5.2.

Table 5.2 Meteorological sensor data for station UNB1.

Parameter	Manufacturer	Model	Range	Accuracy
Temperature	ParoScientific	Met3a	-50 to +60 °C	± 0.1 °C
Relative Humidity	ParoScientific	Met3a	0 to 100%	± 2% RH
Barometric Pressure	ParoScientific	Met3a	620 to 1100 mbar	± 0.08 mbar

Each parameter is logged every 3 minutes.

Meteorological data is logged directly at CACS stations HLFX and FRED. Detailed specifications, as per the manufacturer under ideal circumstances (Casey, 2005), for meteorological sensors used at CACS stations are presented in Table 5.3.

Table 5.3 Meteorological sensor data for CACS stations FRED and HLFX.

Parameter	Manufacturer	Model	Range	Accuracy
Temperature	OMEGA	YSI 44212	± 50.0 °C	± 0.2 °C
Relative Humidity	VAISALA	HMP45A	0.8 to 100%	± 1% RH
Pressure	VAISALA	PTB100A	805 to 1055 mbar	± 0.3 mbar

No meteorological data from HLFX or FRED was archived for the purposes of this research project but is available from the administrators of the CACS program.

5.1.3 GEM Regional Model Data

The GEM regional model generated by the CMC was used to test the validity NWP data for the modeling of zenith tropospheric delay of the GPS signal. In the tests, analysis and forecast model data was accessed. Although forecast data for up to 48 hours from the model initiation time was available, only 12 hours of forecast data was used. This cut-off was chosen so that only the most recent forecast data would be employed in the model. The meteorological parameters of temperature, specific humidity, geopotential height, and pressure at mean sea level were extracted from the model to determine tropospheric delay.

GEM global model data output is made available to the public via the World Wide Web in GRIB format. GEM regional model data output is only made by special agreement with the CMC. This is a globally accepted file data format for the distribution

of gridded meteorological data, such as NWP model output. The World Meteorological Organization has issued 3 editions of the standard. The most current edition is GRIB Edition 2, which is in the process of being phased into use in Europe and the United States. The CMC currently employs GRIB Edition 1, which remains an official standard into the foreseeable future. The GRIB format allows users to access numerical data directly from weather models for post processing and visualization purposes (Canadian Meteorological Centre, 2002).

Data in GRIB format can be decoded using freely available software such as wgrib developed by the National Oceanic and Atmospheric Agency and the National Weather Service. Once the data is decoded, visualization, data extraction, and data format manipulation software such as the Center for Ocean-Land-Atmosphere Studies' Grid Analysis and Display System (GRADS) can be employed. These software products and supporting documentation can be downloaded at http://www.cpc.ncep.noaa.gov/products/wesley/wgrib.html and http://grads.iges.org/grads/ , respectively. The decoded GRIB data is also in a format accessible by the user in any programming language or programming tool. The programs developed for this research project are presented in Section 5.2.1.1.

5.2 Test Data Analysis and Results

The test results presented in the following sections compare the use of a global prediction model and NWP model data in the modeling of zenith tropospheric delay in the measurement and position domains. In the measurement domain, tests were performed on IGS reference station UNB1. Results found using the global prediction model and the NWP model data were compared to GPS derived total troposheric delay values generated by the IGS. In the position domain, tests were performed on the position solution results for the roving GPS receiver on the ferry. The varying distance between each reference station and the ferry is repeated for each crossing. This allows for sampling under similar geometry, but with widely varying atmospheric conditions. Control for the ferry crossing data comes from long / short baseline solution comparisons.

Results show that with the use of NWP model data a significant improvement can be found in the measurement domain. This improvement, however, does not appear to translate into the position domain in this application.

5.2.1 Delays in the Measurement Domain

Zenith tropspheric delay values were determined using the Saastamoinen global prediction model and GEM model data for GPS reference station UNB1. In the

Saastamoinen model, both measured and standard values for temperature, pressure, and relative humidity were used resulting in two delays. The GEM model data was used in an estimation model (see Section 4.3). These calculated delays are compared to GPS derived delays from the IGS final zenith tropospheric delay product in SINEX_TRO format as described in Appendix D. Table 5.4 contains the name and description of each delay shown in the measurement domain comparison results.

Table 5.4 Description of data and models used in tests.

IGS	GPS derived delays from IGS final troposphere zenith path delay product
GEM	Delay estimated from CMC GEM regional model
SAAS	Delays predicted with Saastamoinen model using time series of surface meteorological parameters
SAAS std	Delays predicted with Saastamoinen model using standard surface meteorological parameters

In this case, standard meteorological parameters are considered to be 20 degrees Celsius, 1013.25 millibars pressure, and 50 percent relative humidity.

5.2.1.1 Implementation

A program was written to estimate zenith tropospheric delay from GEM model data. As shown in Table 5.5, along with files containing temperature, specific humidity, pressure, and geo-potential height data extracted from GEM model data, input values of latitude, ellipsoidal height, and geoid-ellipsoid separation values are required for the station to be evaluated.

Table 5.5 Tropospheric delay estimation program input.

Program Input	
File A	Surface Pressure, Temperature, Geo-Potential Height, Specific Humidity extracted from GEM model
File B	Temperature, Specific Humidity, and GeoPotential Height for pressure levels 1015 to 50 millibars
File C	List of pressure levels 1015 to 50 millibars
Station Data	Station Latitude, Ellipsoidal Height, and Geoid-ellipsoid separation (N)

The program generates output of total, wet, and dry zenith tropospheric delay for a single station at a specific time.

The process begins with the determination of barometric pressure at the evaluation station. Barometric pressure at station height cannot be extracted directly from the NWP model since the model is structured as a series of pressure levels. The pressure levels are based on geo-potential height not geometric height. The barometric pressure at the station is estimated based on the surface values of pressure and geo-potential height from the GEM model, as found in File A, and the orthometric height of the station. The process for determining pressure at the station height can be found in Appendix B.

Once the barometric pressure at the station has been determined, the estimation of the zenith tropospheric delay from the station to the upper limit of the GEM model can proceed. As part of the delay estimation process, normal gravity is determined at each pressure level beginning with gravity at station height. The expression for determining normal gravity, along with a list of parameter values used in the equation, can be found in Appendix C.

As presented in Section 4.3, the expression for the estimation of total zenith tropospheric delay is expressed as:

$$ztd = 10^{-6} \int_{p_{ant}}^{p_{top}} k_1 \frac{R_d}{g} dp + 10^{-6} \int_{p_{ant}}^{p_{top}} \frac{R_d}{\in} \left(k_2 - k_1 \in + \frac{k_3}{T} \right) \frac{q}{g} dp \,, \qquad 4.3$$

In equation 4.3, the values for temperature and specific humidity are accessed from File B as taken directly from the GEM model. Refractivity constants from Smith and Weintraub (1953) (as listed in Table 5.6) and values for the mean specific gas constant for dry air, R_d, and water vapour, R_w , (as listed in Table 5.7) from Mendes (1999) are used.

Table 5.6 Refractivity constants from Smith and Weintraub (1953).

k_1	k_2	k_3
77.61 ± 0.01 K mbar^{-1}	72 ± 9 K mbar^{-1}	3.739 ± 0.02 K^2 mbar^{-1}

According to Rueger (2002), alternative determinations of the refractivity constants may be more appropriate in geodetic applications.

Table 5.7 Constants for the specific gas content for dry air and water vapour from Mendes (1999).

R_d	R_w
287.06 ± 0.01 J kg^{-1} K^{-1}	461.525 ± 0.003 J kg^{-1} K^{-1}

A new value for gravity is calculated at each step based on the geometric height of the pressure level.

The total zenith delay is the sum of the delay calculated at the latitude and longitude of the GPS receiver station through each of the 28 layers of the GEM model. The contribution to the total delay above the upper limits of the model was calculated using Saastamoinen global prediction model (see Equations 3.4 and 3.5). The contribution from the atmosphere above the upper pressure level constitutes only a small portion of the total delay, for example, approximately 5 percent of the dry portion of the delay and less than 0.01 percent of the wet delay. The lower limit of the calculated delay is defined by the height of the GPS receiver.

For the tests presented in the next section, a total zenith delay was calculated at every three hours, as limited by the forecast interval of the GEM model, and a cubic spline algorithm was used to generate an hourly result for comparison purposes.

5.2.1.2 Results

The results of the zenith tropospheric delay comparison are shown in terms of zenith total delay. The error has been determined as the difference between the predicted or estimated delay when compared to GPS derived delays from the IGS final tropospheric zenith path delay product.

Total zenith delay values at individual stations are generated based on a weighted least squares estimate of zenith delay through the neutral atmosphere for a global network of IGS reference stations (Gendt and Bevis, 1999). The final product is estimated for every two hours and has an estimated accuracy of 4 millimetres, though; accuracies may vary at individual stations (Gendt, 1999). Weekly files in SINEX_TRO format are available for download at http://igscb.jpl.nasa.gov/components/prods.html. Refer to Appendix D for more information on the SINEX_TRO format. See Bevis *et al*. (1992) for more information on how zenith wet delay, and thereby integrated water vapour, can be estimated from GPS observations.

Statistics have been generated for four periods representative of weather conditions in the winter, spring, summer, and fall. Each period contains variations in temperature, relative humidity, and pressure typical of the season. Detailed graphs of the temperature, relative humidity, and pressure at GPS stations for the evaluation periods can be found in Appendix E. Delay differences generated for each test period at station UNB1 can also be seen in histogram format in Appendix H.

The first evaluation period is day 48 to 51 year 2004 from hour 0 UTC February 17 to hour 24 UTC February 20, 2004. During this period, the weather conditions varied from –17 to 3 degrees Celsius with relative humidity and atmospheric pressure varying with the passing of a storm front. The zenith tropospheric total delay values for this period are shown in Figure 5.2.

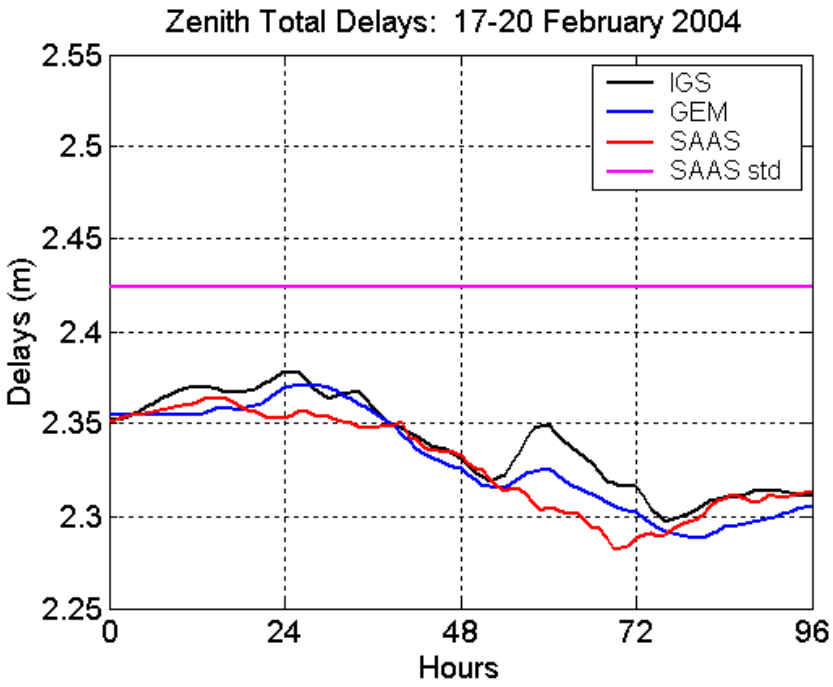

Figure 5.2 Zenith total tropospheric delay values determined for days 48 to 51 at GPS reference station UNB1.

The one sigma Root Mean Square (RMS) error of the difference between the IGS delays minus the GEM delays is 11.8 millimetres over the four day period. The RMS error at one sigma of the IGS delays minus the Saastamoinen with measured and standard meteorological parameters are 17.4 and 87.8 millimetres respectively. The IGS, GEM, and SAAS delays agree well throughout the period. The standard atmospheric values used in the SAASstd delay are clearly not indicative of the conditions. The relatively small total delay values are indicative of the low temperatures, and thereby low water vapour pressure, typically found in the winter season at these latitudes.

The second evaluation period is day 144 to 149 in year 2004 from hour 0 UTC May 23 to hour 24 UTC May 28, 2004. During this period, the weather conditions averaged slightly above zero degree Celsius temperatures with relative humidity remaining above 50 percent. The zenith tropospheric total delay values for this period are shown in Figure 5.3.

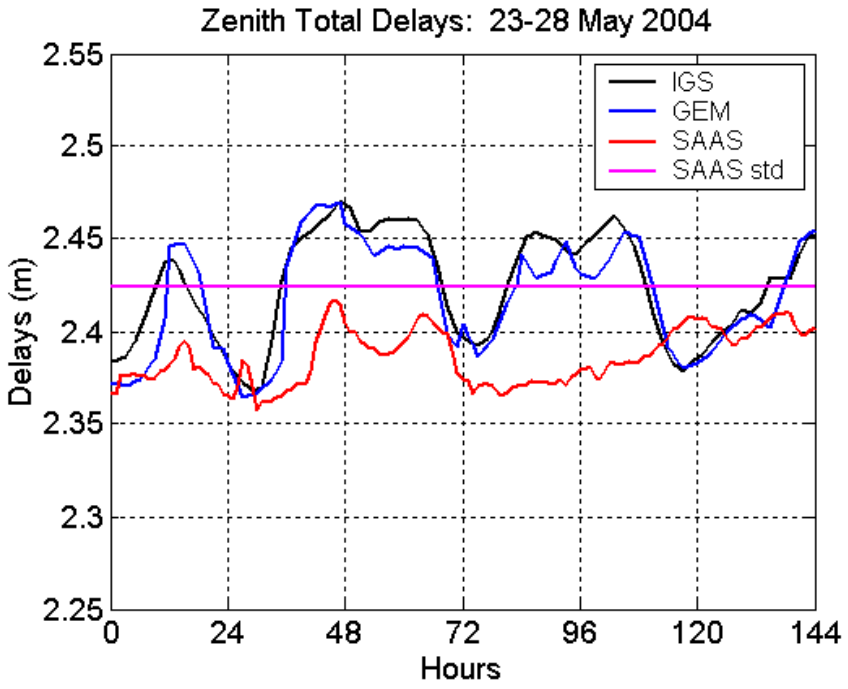

Figure 5.3 Zenith total tropospheric delay values determined for days 144 to 149 at GPS reference station UNB1.

The one sigma RMS error of the differences between the estimation model with the GEM data and the GPS derived delays from the IGS are 13.9 millimetres over the six day period. The RMS error results for the Saastamoinen prediction model with measured

and standard meteorological parameters were 48.8 and 28.8 millimetres, respectively. Here we see a bias in the SAAS delays with respect to the IGS and GEM values throughout most of the evaluation period. It is not clear why the Saastamoinen model displays this degree of inaccuracy with the measured meteorological parameters. It is also interesting to note how well the SAASstd delays represent the average conditions during this period.

The third evaluation period is day 229 to 232 year 2004 from hour 0 UTC August 16 to hour 24 UTC August 19, 2004. The weather conditions during this period are typical with temperatures of approximately 10 degrees Celsius overnight and 30 degrees Celsius daytime highs with relative humidity in the range of 50 to 100 percent. The zenith tropospheric total delay values for this period are shown in Figure 5.4.

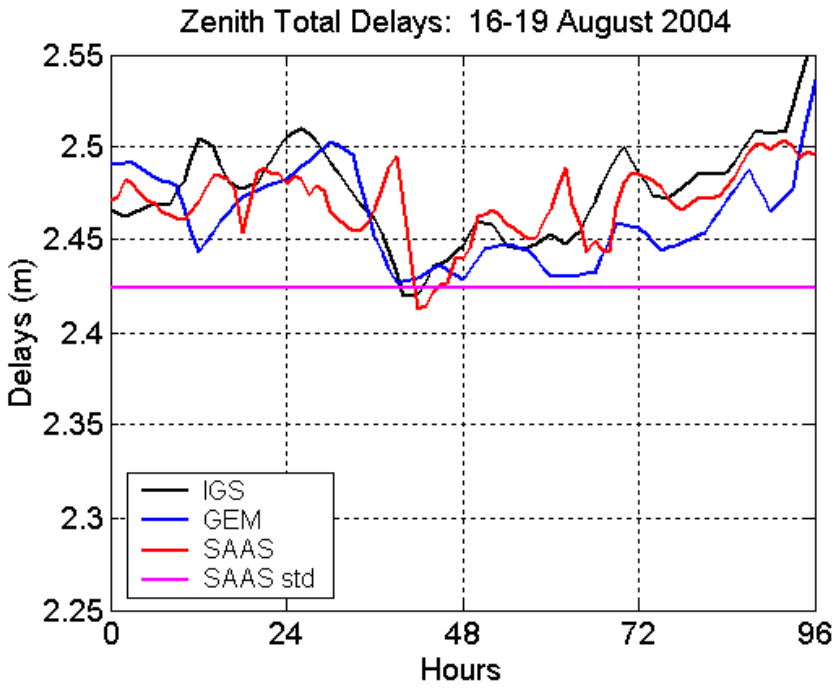

Figure 5.4 Zenith total tropospheric delay values determined for days 229 to 232 at GPS reference station UNB1.

The one sigma RMS error of the differences between the estimation model with the GEM data and the GPS derived delays from the IGS are 22.5 millimetres over the four day period. The RMS error results for the Saastamoinen prediction model with measured and standard meteorological parameters were 19.7 and 56.7 millimetres, respectively. The higher temperatures, and thereby higher water vapour pressure, result in larger delay values in the summer season. The IGS, GEM, and SAAS models agree well during this period.

The fourth evaluation period is day 262 to 264 year 2004 from hour 0 UTC September 17 to hour 24 UTC September 20, 2004. During this period, the weather

conditions averaged 15 to 20 degrees Celsius with relative humidity generally varying between 80 and 100 percent. The zenith tropospheric total delay values for this period are shown in Figure 5.5.

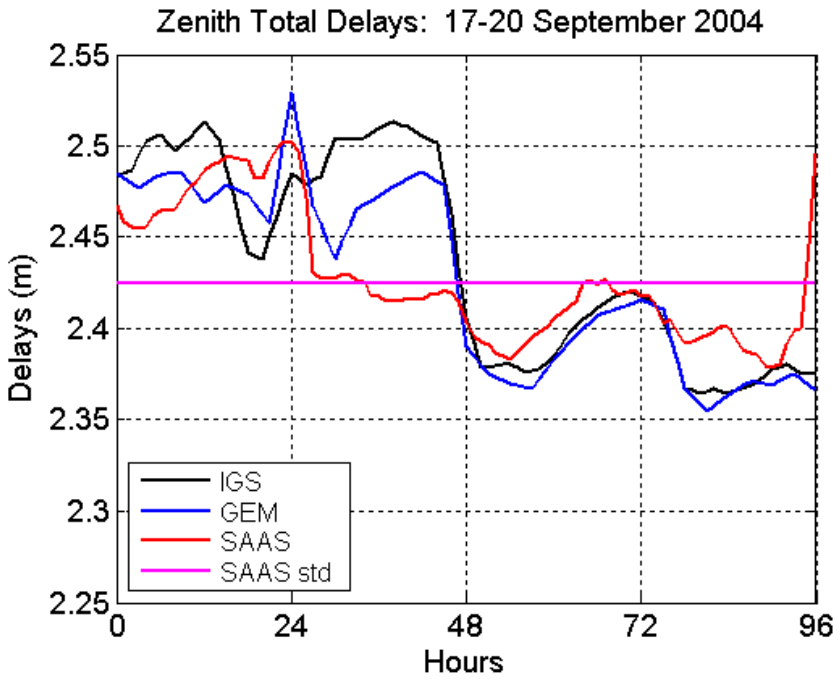

Figure 5.5 Zenith total tropospheric delay values determined for days 262 to 264 at GPS reference station UNB1.

The one sigma RMS error of the differences between the estimation model with the GEM data and the GPS derived delays from the IGS are 22.1 millimetres over the four day period. The RMS error results for the Saastamoinen prediction model with measured and standard meteorological parameters were 45.0 and 56.9 millimetres, respectively.

Data assimilation for the GEM model results in an analysis rather than a forecast at 12 and 0 hours UTC each day. No obvious improvement is seen with the use of the analysis over the forecast values in the determination of the delay. This indicates that the 12 hour forecast cycle may be sufficient to ensure an improved estimated delay throughout the day not just at or near the times of the analysis.

The standard deviations, mean, and RMS error at one sigma level for all the modelled delays determined at UNB1 compared to GPS derived total tropospheric delays computed by the IGS are given in Tables 5.8.

Table 5.8 Standard deviation, mean and RMS (in millimetres) of differences in zenith delays for station UNB1. IGS minus modelled delays.

Day	RMS Error in Estimation of zenith tropospheric delay (mm)								
	IGS – NWP			IGS – SAAS			IGS – SAAS std		
	St.Dev.	Mean	RMS	St.Dev.	Mean	RMS	St.Dev.	Mean	RMS
48-51	6.5	9.9	11.8	14.2	10.3	17.4	24.7	-84.3	87.8
144-149	12.5	6.2	13.9	29.5	38.9	48.8	28.9	0.5	28.8
229-232	18.1	13.5	22.5	19.8	0.7	19.7	25.6	50.7	56.7
261-264	19.2	11.1	22.1	44.1	10.2	45.0	55.5	14.0	56.9

The results show a consistent and significant improvement in estimated zenith total delay with the use of NWP model data. These results are consistent with previous findings from other researchers (Jensen, 2002c; Jupp *et al*., 2003; Bisnath *et al*., 2004). In only one case, days 229 to 232, the RMS error value for the Saastamoinen model with

measured meteorological parameters resulted in a lower value than the GEM model delay. This indicates that the GEM model delays are more reliable than those estimated with the Saastamoinen global tropopheric prediction model. Results divided by day can be seen in Appendix F. Total delay comparisons during the test periods for station CGSJ can be seen in Appendix G. The tests in Section 5.2.2 will demonstrate whether a significant improvement can be obtained in the positioning results due to this improvement in the measurement domain.

5.2.2 Effect of Delays in the Position Domain

The GPS data files used for the positioning tests incorporate delays estimated using the GEM model (GEM), delays predicted with the Saastamoinen model with measured surface meteorological parameters (SAAS), and delays predicted with the Saastamoinen model using standard surface meteorological parameters (SAAS std). All processing was performed with DynaPos software provided by the XYZs of GPS.

5.2.2.1 Implementation

DynaPos is a GPS positioning software that was developed with real-time kinematic applications in mind. It employs both real-time and playback processing

styles. Real-time capabilities are available when the software is used in conjunction with a GPS Receiver Interface Module (GRIM). The playback mode is actually an exact replica of events that would have occurred in real-time but played back in post-processing. The following paragraphs will outline some of the other main features and capabilities available with the software.

DynaPos uses a Kalman filter algorithm to process GPS data in order to solve for position. Remondi and Brown [2000] describes the Kalman filter algorithm used in DynaPos. Essentially, it is capable of forming pseudorange and carrier-phase double-differences and carrier-phase triple differences. The user is free to set the parameters associated with the filter, such as code and carrier standard deviations, as required. It also allows for the user to define a reference solution in such a way that the Kalman filter can provide an error estimate. DynaPos processes L1 code, L1 carrier, L2 code, and L2 carrier data types in various data combinations. As can be seen in Table 5.9, each data combination is designed to provide an optimum solution for a particular positioning situation.

Table 5.9 Data combinations available for DynaPos processing.

Data Combination	Integer Fixing	Purpose
L1 Carrier	Yes	Calibration and Short Baselines
L1 Code	No	Calibration and Short Baselines
L2 Carrier	No	Calibration and Short Baselines
L2 Code	No	Calibration and Short Baselines
L1 Carrier & L1 Code	Yes	Short BLs & Quicker Convergence
L2 Carrier & L2 Code	No	Short BLs & Quicker Convergence
L1+L2 (narrow lane) Carrier	Yes	Short BLs, Accuracy, Integrity
L1+L2 Code	No	Robust/ accurate mid-BL Positioning
L1+L2 (narrow lane) Carrier & L1+L2 Code	Yes	Short BL, Quick Start, Accuracy, Integrity
Iono-free Carrier	No	Long BLs
Iono-free Code	No	Long BLs
Iono-free Carrier & Iono-free Code	No	Accuracy, Quick Start, for Long BLs
Iono-free Carrier & L1+L2 Code	No	Accuracy for long BLs, Quick Start
L1-L2 (wide lane) Carrier	Yes	Integer Monitoring & Fixing, Quick Start, Integrity
L1-L2 (wide lane) Carrier & L1+L2 Code	Yes	Integer Monitoring & Fixing, Integrity

The user is free to switch between data combinations, as required during both the real time and playback processing modes. Integer ambiguity fixing capabilities are available for some data combinations and can also be turned on and off during processing. Windows are available during the real-time and playback sessions to monitor and interact with the processing. These include a baseline processing status window, integer ambiguity status window, data channel status window, engine processing status window, Kalman filtering pre-processing status window, Kalman filtering processing status window, error estimates and sigma plot window, real-time motion plot window, satellite visibility window, steering window, and heading display window. Figure 5.6 shows the

baseline processing status window, integer ambiguity status window, and the satellite visibility window during a playback session.

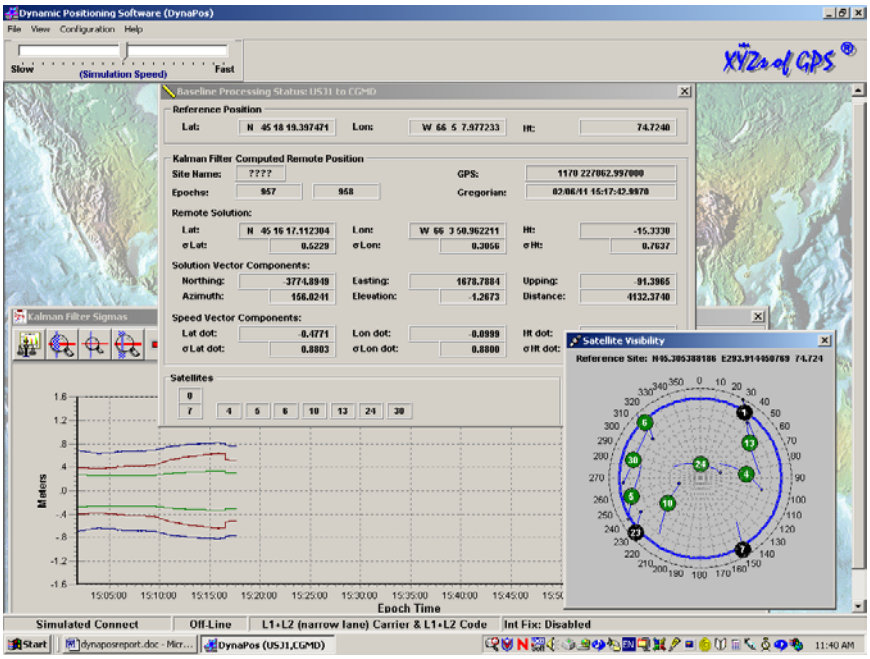

Figure 5.6 Example of processing windows.

DynaPos accepts GPS data in several formats. In real-time processing mode, each receiver is connected to a PC or laptop running the GRIM software. The GRIM accepts raw data from the receiver and then pipes it to DynaPos in an acceptable format. Raw data from Ashtech, Leica, Novatel and Trimble receivers is currently supported. Input data for the playback processing must be in RINEX or Ashtech B/E file formats.

The processed results are available in three output formats: Remote Position files (X file), Remote Trajectory files (Y file), and DynaPos Debug files (Z file). Each of these files contains per epoch position solutions and associated standard deviations, as

well as associated ancillary data. The Remote Trajectory output file is optional and the Debug file can be adjusted to provide varying degrees of processing detail. All output files are in a convenient format that can be viewed with any text editor.

Obtainable positioning accuracies are in the sub-centimetre or low centimetre level for short baselines (ambiguity fixed solution for baselines up to 10 kilometres), in the centimetre level for mid length baselines (baselines in the 10 to 40 kilometres range) and in the decimetre level for long baselines (baselines in the 40 to 100's kilometres range). Solutions can be derived for baselines hundreds of kilometres long.

DynaPos is a powerful GPS processing tool that can be used for both real-time and post-processing application. The overview presented in this Section was intended to be a general outline of some of the main features and was not meant to be inclusive of all the features and capabilities of the DynaPos software. The interested reader should refer to the DynaPos User's Manual [*The XYZs of GPS*, 2001] for further details concerning the features discussed in this Section.

All results shown in this report were processed using one of two data processing techniques, ionospheric delay-free carrier and code or integer ambiguity fixed narrow-lane, in the playback or post-processing mode. The ionospheric delay-free carrier and code processing mode is shown as it provides a relatively risk free solution that minimizes the effect of the errors associated with the ionosphere. This mode does not employ integer fixing and can result in an extended time for convergence (Cove and Santos, 2004). The narrow-lane integer fixed process allows the user to achieve both a

higher accuracy solution, as well as, specific goals such as quick convergence. All data was post-processed with a 10 degree elevation mask and precise orbits.

The positioning tests were performed in such a way that any improvements in position solution should be directly related to the handling of the tropospheric delay. This was done by applying the hydrostatic and wet delays estimated from the methods described in Section 5.2.1 directly to the RINEX observation files for the GPS stations CGSJ and BOAT. The hourly delays were interpolated using a cubic spline algorithm to one second to match the one hertz GPS data. The Niell mapping function was applied to map the zenith delays to the appropriate elevation angle to generate slant delays. The slant delays were subtracted from the raw code and phase observations in the RINEX file. Each version of the modified RINEX files were then processed using the ionospheric delay free linear combination to generate long baseline kinematic solutions for BOAT station. Each long baseline solution was then evaluated with respect to a narrow-lane, fixed ambiguity short baseline solution between DRHS and BOAT. The Rinex files in processing the short baseline did not have estimated delays applied. It should be noted that applying the estimated delays to the RINEX files is not an ideal solution to this situation; ideally, the delays would be applied directly during processing. This was not possible due to the use of commercial processing software where the source code would not be made available for the required modifications.

It must be noted that no measures beyond double differencing and the use of the ionospheric delay free processing were applied to the observations in order to address

residual effects from the ionosphere or multipath. Residual effects from these error sources may continue to contribute to the error budget of the position solutions.

5.2.2.2 Results

Position domain tests were performed on selected time series from the test periods identified in the measurement domain tests shown in Section 5.2.1. These time series were selected based on several criteria, namely, the weather and the location of the ferry. The time series were meant to represent periods of weather that were highly correlated and highly de-correlated over the test area (i.e. during the passage of a weather front). In other words, times when the weather was the same over the test area and times when the weather varied greatly over the test area. This was done in order to show if the use of the NWP model data would be beneficial in situations were there is significant differential troposphere, little differential troposphere, in both cases, or not beneficial in any case. Substantial differential troposphere, such as during the passage of weather fronts, can be associated with degraded position results; therefore, this was of particular interest (Gregorius and Blewitt, 1998). The second criterion was to choose times where the ferry was docked in Digby. This provided a kinematic data set, but does not add in the additional complication of not being able to achieve a high accuracy, fixed ambiguity solution, as the baseline between DRHS and BOAT never exceeds 5 kilometres.

The statistics given in Table 5.10 are based on solution differences between the short baseline solution between DRHS and BOAT (approximate distance of 4 kilometres) and the long baseline solution between CGSJ and BOAT (approximate distance of 74 kilometres).

Table 5.10 Standard Deviation (m) for kinematic data sets. Short baseline solution minus long baseline solution.

Day	Hour UTC	RMS error in position from ionospheric delay free solution compared to narrow lane fixed solution (in cm).					
		NWP		SAAS		SAAS std	
		Horizontal RMS	Vertical RMS	Horizontal RMS	Vertical RMS	Horizontal RMS	Vertical RMS
49	1800-2000	15.03	7.87	8.04	13.90	7.57	10.40
51	1800-2000	6.32	14.90	4.68	17.10	5.22	12.50
146	0700-1000	5.31	8.00	5.60	6.40	5.45	6.60
148	0700-1000	10.28	6.00	9.00	7.90	10.32	7.00
229	2245-2345	31.68	41.70	4.67	11.10	3.04	14.30
230	0700-0800	17.36	22.70	20.46	11.90	19.56	13.80
261	1500-1600	6.21	7.50	5.75	18.30	6.30	5.20
263	1500-1600	12.62	19.70	12.42	14.20	12.79	19.80

Time series on days 49, 146, 230, and 263 represent times where weather conditions, particularly barometric pressure, varied over the test area. The remaining time series, 51, 148, 229, and 261, represent times where the weather conditions over the test area were well correlated. No significant improvements in positioning results are found in either case and, in fact, no one solution provides the best solution in all cases. The continuity in the position results using the different modeled delays could be attributed to a lack of significant differential troposphere. The reference stations CGSJ and BOAT do not differ greatly in height and the baseline is only 75 kilometres. If there were a great difference in the heights of the reference stations, longer baselines, or extremely

decorrelated weather over the test area the resulting differential troposphere may have resulted in a significant improvement in position solution using the GEM model delays (Jensen, 2002c). The inconsistency found on day 229 does may be due to the use of forecast data very late in the 12 hour forecast cycle. No significant discrepancy, however, appears in the measurement domain (see Figure 5.3) between the GEM and IGS delays at station UNB1 that would explain the large difference in RMS error found in the position domain during this time period.

One can conclude that based on these position domain results, the Saastamoinen global prediction model with standard meteorological parameters is as effective or more effective than employing additional measures such as NWP model data or measured meteorological parameters. The improvement found in the measurement domain does not translate significantly into the position domain for this time series of data.

6 CONCLUSIONS AND RECOMMENDATIONS

The modeling of tropospheric delay remains a significant source of error in differential GPS positioning. Several methods for improving the estimation of the delay have been proposed, including the use of Numerical Weather Prediction models.

The objective of this thesis was to investigate the use of a NWP model in the modelling of zenith tropospheric delay. Zenith delays estimated with NWP model data were compared to delays computed with a global prediction model in the measurement and position domains. A significant improvement was found in the measurement domain with the use of NWP model data over a global prediction model in the estimation of tropospheric delay for the GPS reference station UNB1. This improvement did not translate into an improvement in the position domain for a 75 kilometre baseline between the roving GPS station BOAT and reference station CGSJ.

In the measurement domain, zenith total tropospheric delays were estimated from Regional GEM NWP model data and the Saastamoinen global prediction model, with measured and standard atmospheric parameters, for four distinct time periods over one year. The delays were compared to GPS derived final zenith path delay product produced by the IGS for GPS reference station UNB1. The results show significant improvement in zenith tropospheric delay estimation with use of NWP model data. The delays estimated with GEM model data were found to agree with the IGS delays with a RMS error in the range of 11.8 to 22.5 millimetres. This is an improvement on the delays estimated with Saastamoinen global prediction model both with the use of

measured and standard atmospheric parameters. The resulting delays for the prediction model with measured and standard parameters as compared to the IGS delays had a RMS error in the range of 17.4 to 48.8 millimetres and 28.8 to 87.8 millimetres, respectively. The NWP model data consistently produced delay results that were superior to those produced with the Saastamoinen global prediction model.

Tropospheric delays were then estimated for a network of GPS stations in and around the Bay of Fundy. The NWP and prediction model delays were applied to GPS data in order to evaluate the effect in the position domain. No apparent improvement was found with the use of NWP delays over the use of the traditional global prediction model. In fact, in one case on day 229 a significantly worse position solution was produced by the NWP model data. There was also no apparent improvement with use of surface meteorological data in the global tropospheric prediction model over the use of standard meteorological parameters.

The lack of improvemnent in the position solution can perhaps be attributed to the homogeneity of weather conditions over area during the test periods resulting in a lack of differential troposphere between the stations. Additionally, the reference stations did not vary greatly in terms of height and the baseline evaluated may not have been sufficiently long to show any significant improvements in position error due to improved modeling of the tropospheric delay.

Results in zenith delay estimation and positioning are promising but require further study. Improvements may be found in areas not investigated in this research

including the impact on ambiguity resolution and network rather than single baseline applications. Suggestions for some future work are outlined below.

Study in this area of research would benefit from the inclusion of longer baselines and more varied weather conditions. In this particular research project, the tests could be expanded to include stations in Fredericton and Halifax giving baseline distances up to 200 kilometres.

Several other aspects of the research should be addressed in future work. One of these was how the estimated delays were applied to the GPS data. Ideally, the delays would be estimated during processing rather than applying them to the Rinex file prior to processing. This could be easily accomplished with the use of processing software with accessible code. Another useful exercise would be to ray trace through the NWP rather than determining the zenith delay in order to evaluate the potential benefits on low elevation angles. Finally, some researcher have found improvements can be found in ambiguity resolution with NWP model data.; it would be useful to evaluate whether this is the case with this data set.

Research into the use of NWP models for GPS positioning is a relatively new area. Extensive testing in time, coverage, and weather conditions is required in order to fully explore the potential of the use of NWP in this application. This thesis represents an initial investigation into the use of the Canadian Regional GEM model for GPS positioning.

LIST OF REFERENCES

Barry, R.G. and R.J. Chorley (1998). *Atmosphere, Weather, and Climate*. 7th Ed., Routledge, London.

Bisnath, S., D. Dodd, and M.P. Cleveland (2004a). "Analysis of the Utility of NOAA-Generated Tropospheric Refraction Corrections for the Next Generation Nationwide DGPS Service." Proceedings of ION GNSS 2004, Long Beach, CA, September 21-24.

Bisnath, S., D. Wells, M. Santos, and K. Cove (2004b). "Initial Results from a Long Baseline, Kinematic, Differential GPS Carrier Phase Experiment in a Marine Environment." PLANS 2004, Monteray, California, 26-29 April 2004.

Bock, O. and E. Doerflinger (2001). "Atmospheric Modeling in GPS data Analysis for High Accuracy Positioning." *Physics and Chemistry of the Earth*, Vol. 267, No. 6-8, pp. 373-383.

Campbell Scientific (2005). Product Manual. Retrieved 15 January 2005 from World Wide Web.
(http://www.campbellsci.ca/CampbellScientific/Products_Sensors.html)

Canadian Meteorological Centre (2002). Operational Model Forecasts. Retrieved 9 July 2004 from World Wide Web.
http://www.weatheroffice.ec.gc.ca/model_forecast/about_these_products_e.html

Casey, M. (2005). Personal communication. Geodetic Survey Division, Natural Resources Canada, Ottawa, ON, March.

Cove, K., M. Santos, D. Wells, and S. Bisnath (2004). "Improved Tropospheric Delay Estimation for Long Baseline, Carrier-Phase Differential GPS Positioning in a Coastal Environment." Institute of Navigation GNSS 2004, Long Beach, California, USA, 21-24 September 2004.

Cove, K. and M. Santos (2004). "Initial Results and Future Goals for the Princess of Acadia Project." Presentation for Real-Time Kinematic GPS Navigation for Hydrography Surveys and Seamless Vertical Datums Workshop, Long Beach, Mississippi, USA, 16-18 March 2004.

Gendt, G. and M. Bevis (1998). Some Remarks on New and Existing Tropospheric Products. IGS Workshop Proceedings:1998 Network Systems Workshop, C.E. Noll, K.T. Gowey, R.E. Neilan, eds., Jet Propulsion Laboratory, Pasadena, CA.

Gendt, G. (1999). Status Report of Tropospheric Working Group. Retrieved 9 July 2004 from World Wide Web.
http://www.gfz-potsdam.de/pb1/igs_trop_wg/main_IGS_TROP_WG.html

Gregorius, T. and G. Blewitt (1998). "The Effects of Weather Fronts on GPS Measurements." *GPS World*, Innovation Column, May issue, pp.52-60.

Gutman, S.I., T. Fuller-Rowell, and D. Robinson (2003). "Using NOAA Atmospheric Models to Improve Ionospheric and Tropospheric Corrections." Presented at US Coast Guard Differential GPS Symposium, Portsmouth, Virginia, June 19, 2003.

Han, S. (1997). *Carrier Phase-Based Long-Range GPS Kinematic Positioning*. School of Geomatic Engineering UNISURV Report S-49 , The University of New South Wales, Sydney , Australia.

Hess, S.L. (1979*). Introduction to Theoretical Meteorology*. Reprint ed., Robert E. Krieger Publishing Company, Inc., Florida.

Hofmann-Wellenhof, B., H. Lichtenegger, and J. Collins (1992). *GPS Theory and Practice*. 5th ed., Springer-Verlag Wien, New York.

Hogue, R., G. Croteau, and R. Jones (1998). Operational Runs. Coll. NWP Workshop. Retrieved 24 November 2004 from World Wide Web.
http://www.msc-smc.ec.gc.ca/cmc_library/protected/NWP/e_oprun.htm

Jensen, A.B.O. (2002a). "Numerical Weather Prediction for Kinematic GPS Positioning." Presented at ION GPS 2002, Portland, OR, September 24-27.

Jensen, A.B.O. (2002b). "Investigations on the Use of Numerical Weather Predictions, Ray Tracing, and Tropospheric Mapping Functions for Network RTK." Presented at ION GPS 2002, Portland, OR, September 24-27.

Jensen,A.O. (2002c). "Numerical Weather Prediction for Network RTK." Ph. D. Thesis. Publications Series 4, Volume 10, National Survey and Cadastre, Denmark.

Jupp, A., S. Healy, M. Powe, J. Owen, and J. Butcher (2003). "Use of Numerical Weather prediction for the Improvement of Tropospheric Corrections in Global Positioning Applications." Presented at ION GPS/ GNSS 2003, Portland, OR, September 9-12.

Laroche, S. (1998). Data Assimilation Cycles at the Canadian Meteorological Centre. Coll. NWP Workshop. Retrieved 24 November 2004 from World Wide Web. http://www.msc-smc.ec.gc.ca/cmc_library/protected/nwp/nwp_e.html

McCarthy, D.D. and G. Petit (2003). IERS Conventions. IERS Technical Note 32.

Mendes, V.B. (1999). Modelling the neutral-atmosphere propagation delay in radiometric space techniques. Ph.D. dissertation. Department of Geodesy and Geomatics Engineering. Technical Report no. 199. University of New Brunswick, Fredericton, New Brunswick.

Misra, P. and P. Enge (2001). *Global Positioning System Signals, Measurements, and Performance*. Ganga-Jamuna Press, Lincoln, Massachusetts.

Niell, A. E. (1996). Global mapping functions for the atmospheric delay at radio wavelengths. *Journal of Geophysical Research*. Vol. 101, no. B2, pp. 3227-3246. The American Geophysical Union.

Pany, T., P. Pesec, and G. Stangl (2001a). "Atmospheric GPS Slant Path Delays and Ray Tracing Through Numerical Weather Models, a Comparison." *Physics and Chemistry of the Earth*, Vol. 26, No. 3, pp.183-188.

Pany, T., P. Pesec, and G. Stangl (2001b). "Elimination of Tropospheric Path Delays in GPS Observations with the ECMWF Numerical Weather Model." *Physics and Chemistry of the Earth*, Vol. 26, No. 6-8, pp.487-492.

ParoScientific, Inc. (2004). Met3a Meteorological System. Retrieved 15 January 2004 from World Wide Web. (http://www.paroscientific.com/met3a.htm)

Remondi, B. and G. Brown (2000). "Triple Differencing with Kalman Filtering: Making It Work." *GPS Solutions*, Vol. 3, No. 3, pp. 58-64.

Rueger, J.M. (2002). "Refractive Index Formulae for Radio Waves." FIG XXII International Congress, Washington, D.C., April 19-26, 2002.

Saastamoinen J. (1973). "Contributions to the Theory of Atmospheric Refraction." *Bulletin Geodesique,* 105, pp.279-298, 106, pp. 383-397, 107, pp. 13-34. Printed in three parts.

Santos, M. C., N. C. C. Silva and L. C. Oliveira. (2000). "An assessment on the effect of tropospheric delay on geodetic positioning using GPS data collected by the RBMC network." *Advances in Space Dynamics*, Antonio F. B. A. Prado (Ed.), National Institute of Space Research, São José dos Campos, SP, Brazil, pp. 447-455.

Santos, M., D. Wells, K. Cove, and S. Bisnath (2004). " The Princess of Acadia GPS Project: Description and Scientific Challenges." Canadian Hydrographic Conference, Ottawa, Ontario, Canada, 24-27 May 2004.

Shueler, T., G.W. Hein, and B. Eissfeller (2000). "Improved Tropospheric Delay Modelling Using an Integrated Approach of Numerical Weather Models and GPS." Presented at ION GPS 2000, Salt Lake City, UT, September 19-22.

Smith, E.K. and S. Weintraub (1953). "The constants in the equation for atmospheric refractive index at radio frequencies." Proceedings of the Institute of Radio Engineers, Vol. 4, pp. 1035-1037.

Thayer, G.D. (1974). "An improved equation for the radio refractive index of air." *Radio Science*, Vol. 9, No. 10, pp. 803-807.

The XYZs of GPS (2001). "DynaPos^{TM} GPS Real-Time Dynamic Positioning Software User's Manual." The XYZs of GPS, Inc., Dickerson, MD.

Tsujii, T., J. Wang, L. Dai, C. Rizos, M Harigae, T. Inagaki, T. Fujiwara, and T. Karo (2001). A Tachnique for Precise Point Positioning of High Altitude Platforms System (HAPS) Using a GPS Ground Reference Network. In Proceedings of ION GPS 2001, pp. 1017-1026.

Vedel, H. (2000). Conversion of WGS84 geometric heights to NWP model HIRLAM geopotential heights. DMI scientific report 00-04, Danish Meteorological Institute.

Vedel, H., K.S. Mogenson, and X. -Y. Huang (2001). "Calculation of Zenith Delays from Meteorological Data Comparison of NWP Model, Radiosonde and GPS Delays." *Physics and Chemistry of the Earth*, Vol. 26, No. 6-8, pp.497-502.

Wallace, J.M., and P.V. Hobbs (1977). *Atmospheric Science, an Introductory Survey*. Academic Press Inc.

Wells, D.E., N. Beck, D. Delikaraoglou, A. Kleusberg, E.J. Krakiwsky, G. LaChapelle, R.B. Langley, M. Nakiboglu, K.P. Schwarz, J.M. Tranquilla, and P. Vanicek (1986). *Guide to GPS Positioning*. Department of Geodesy and Geomatics Engineering Lecture Note No. 58, University of New Brunswick, Fredericton, New Brunswick, Canada, 291 pp.

Wells, D., S. Bisnath, S. Howden, D. Dodd, M. Santos, K. Cove, D. Kim, and B. Remondi (2004). "Prospects for Extended-Range Marine PPK." International Navigation Conference MELAHA 2004, Cairo, Egypt, 13-15 April 2004.

BIBLIOGRAPHY

Bevis, M., S. Businger, T.A. Herring, C. Rocken, R.A. Anthes, and R.H. Ware (1992). "GPS Meteorology: Remote Sensing of Atmospheric Water Vapour sing the Global Positioning System." *Journal of Geophysical Research,* Vol. 97, No. D14, pp. 15,787-15,801.

Davis, J.L., T.A. Herring, I.I. Shapiro, A.E. Rogers, and G. Elgered (1985). Geodesy by radio interferometry: Effects of atmospheric modeling errors on estimates of baseline length. *Radio Science*. Vol. 20, no. 6, pp. 1593-1607.

De Haan, S., and H. van der Marel (2004). "The influence of GPS estimates of NWP-derived mapping functions." *Physics and Chemistry of the Earth*, 29, pp. 159-166.

De Haan, S., H. van der Marel and S. Barlag (2002). "Comparison of GPS slant delay measurements to a numerical model: case study of a cold front passage." *Physics and Chemistry of the Earth*, Vol. 27, pp. 317-322.

Dodson, A. H., P. J. Shardlow, L. C. M. Hubbard, G. Elgered and P. O. J. Jarlemark (1996). "Wet tropospheric effects on precise relative height determination." *Journal of Geodesy*, Vol. 70, pp. 188-202.

Han, S., and C. Rizos (1997). "Comparing GPS ambiguity resolution techniques." *GPS World,* Vol. 8, No. 10, pp. 54-61.

Langley, R. (1995). Propagation of the GPS Signals. GPS for Geodesy, Netherlands Geodetic Commission, Delft, The Netherlands. Edited by Kleusberg, A. and P.J.G. Teunissen.

Mendes, V.B. and R.B. Langley (1995). "Zenith Wet Tropospheric Delay Determination Using Prediction Models: Accuracy Analysis." *Cartografia Cadastro*, No. 2, Junho, pp. 41-47.

Niell, A.E. (2001). "Preliminary Evaluation of Atmospheric Mapping Functions Based on Numerical Weather Models." *Physics and Chemistry of the Earth*, Vol. 26, No. 6-8, pp.475-480.

Vedel, H., and X.-Y. Huang (2004). "A NWP study with ground based GPS data." Geophysical Research Abstracts, Vol. 6, 02908, 2004.

Walpersdorf, A., E. Calais, J. Hasse, L. Eymard, M. Desboie and H. Vedel (2001). "Atmospheric Gradients Estimated by GPS Compared to a High Resolution Numerical Weather Prediction (NWP) Model." *Physics and Chemistry of the Earth*, Vol. 26, No. 3, pp.147-152.

APPENDIX A - Coordinates of GPS stations in ITRF and NAD83 (CSRS)

Table A.1 ITRF station coordinates (in degrees – minutes - seconds and metres).

Station	Latitude	Longitude	Height (m)
UNB1	45-57-00.7525	66-38-30.1359	22.8469
CGSJ	45-16-17.5436	66-03-46.6853	4.568
DRHS	44-37-13.7901	65-45-34.9658	37.469
FRED	45-56-0.6237	66-39-35.5646	94.84
HLFX	44-41-0.7765	63-36-40.6031	3.11

Table A.2 NAD83 station coordinates (in degrees/ minutes/ seconds and metres).

Station	Latitude	Longitude	Height
UNB1	45-57-0.7145	66-38-30.1376	23.9659
CGSJ	45-16-17.5082	66-03-46.6831	5.710
DRHS	44-37-13.7550	65-45-34.9643	38.633
FRED	45-56-00.5889	66-39-35.5646	95.96
HLFX	44-41-00.7422	63-36-40.6073	4.28

APPENDIX B – Description of the process for determining station barometric pressure for use in the estimation of tropospheric delay with NWP model data

A process is used to determine station barometric pressure from surface NWP model data (Gutman *et al*., 2003). NWP models are based on pressure rather than height. In order to determine zenith total delay from the NWP model, one must first determine pressure at the station height. This can be performed with surface pressure and geopotential height data contained in the NWP model and the orthometric height of the station. The pressure at mean sea level, or Altimeter Setting (*AS*), at a station location can be expressed as:

$$T_1 = (Psfc^{0.1903} + 1.313 * 10^{-5} * Hsfc)^{5.255}, \quad \text{B.1}$$

$$AS = T_1 * 33.86429, \quad \text{B.2}$$

where *Psfc* is the pressure at the earth's surface in inches, *Hsfc* is the geopotential height of the earth's surface in feet, and the pressure at mean sea level is in millibars. The pressure at the station, or *Psta*, can then be determined with the following expression:

$$Psta = (T_1^{1/0.1903} - (1.313 * 10^{-5} * Hsta))^{1/5.255} * 33.86429, \quad \text{B.3}$$

where *Hsta* is the height of the orthometric station in feet and the pressure at the station is in millibars.

For he interested reader, the process for converting geometric heights to geopotential heights is described in Vedel (2000).

APPENDIX C – The expression for determination Normal Gravity

Normal gravity should be evaluated at the GPS station and at each layer in the NWP model. The following are a list of the equation components and constants used to evaluate normal gravity in the program for determining zenith tropospheric delay as described in Section 5.2.1.1.

Table C.1 List of equation values and constants used in the determination of normal gravity.

Parameter	Value	Reference
Ge	9.7803267715	Normal gravity at equator in m/ s^2
k	0.001931851353	Relation between normal gravity and ellipsoidal axis
f	1/298.257222100883	Ellipsoidal flattening, GRS80
e2	0.0066943800299	Ellipsoidal second eccentricity
A1	3.0877*10^-6	Constant from series expansion to the order of f
A2	0.00142	Constant from series expansion to the order of f
A3	0.75*10^-12	Constant from series expansion to the order of f

The expression for normal gravity (Torge, 1989) at the surface of the ellipsoid is expressed as:

$$G0 = \frac{Ge*(1+(k*\sin^2(Lsta)))}{\sqrt{(1-(e2*\sin^2(Lsta))}}, \qquad \text{C.1}$$

Where *Lsta* is the latitude of the station in radians and the G0 is in metres / second^2. The normal gravity at the station, *G*, is expressed as:

$$G = G0 - A1*(1 - A2*\sin^2(Lsta)*Hsta) + A3*Hsta^2, \qquad \text{C.2}$$

where *Hsta* is the geometric height of the station and *G* is in metres / second^2.

APPENDIX D – Description of the SINEX_TRO format

The Solution (Software/technique) INdependent EXchange (SINEX_TRO) format is used for the combination of tropospheric estimates product generated by the IGS. The product contains total zenith path transformed to precipitable water vapour for selected IGS stations. A complete description of the SINEX_TRO format including an example of the Combination Product can be found at the Jet Propulsion Laboratory website at ftp://igscb.jpl.nasa.gov/pub/data/format/sinex_tropo.txt.

The file format is based on the SINEX format containing blocks that include file/reference, site/eccentricity, site/ID, site/antenna/site receiver, site/GPS_phase center. Additional blocks created to hold data and information specific to the troposphere estimates are trop/description, trop/sta_coordinates, and tro/solution blocks.

Files containing total zenith path delay parameters are submitted to IGS Analysis Centers for all participating global sites. A water vapour product can be generated for those sites with meteorological data available. Where meteorological data is not available only the zenith path delay product can be generated.

The files archived and available for download on the IGS website are in a weekly file with a separate file for each site. The files contaning only the zenith path delay product are named sssswwww.zpd and those also containing the water vapour product, referred to as the combination product, are named sssswwww.tro (where ssss refers to the station designation and wwww refers to the GPS week).

APPENDIX E - Detailed graphs of the temperature, relative humidity, and pressure at GPS stations UNB1, CGSJ, DRHS, and BOAT for the test evaluation periods

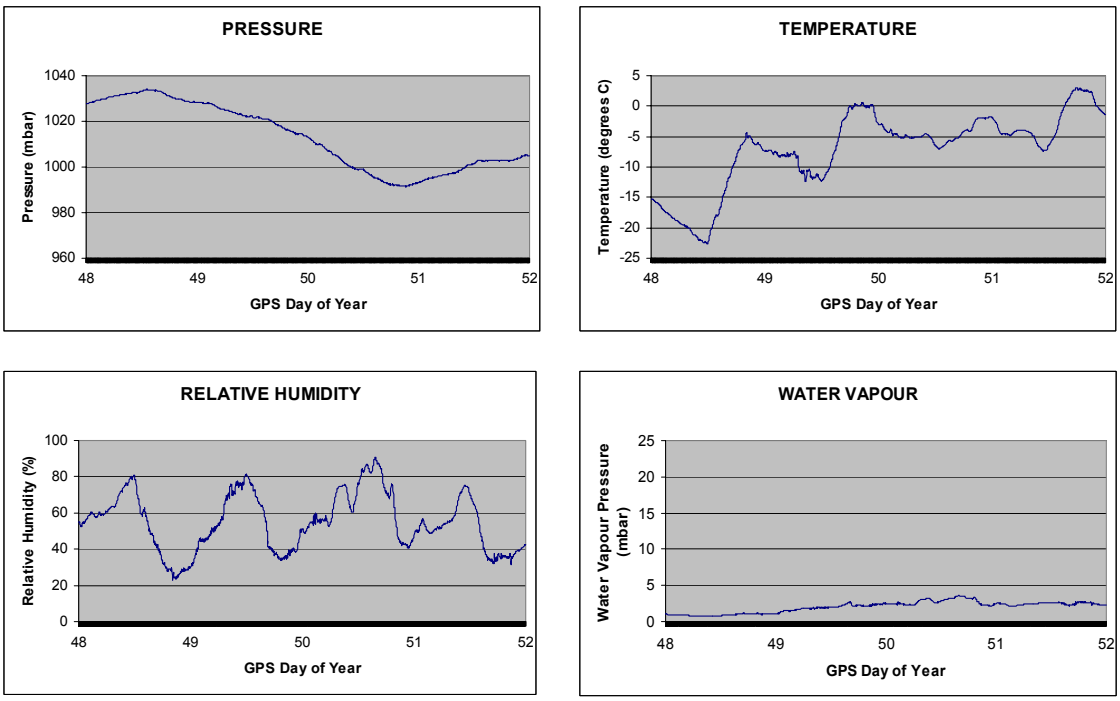

Figure E.1 Pressure, temperature, relative humidity, and water vapour pressure at GPS reference station UNB1 for days 48 to 51.

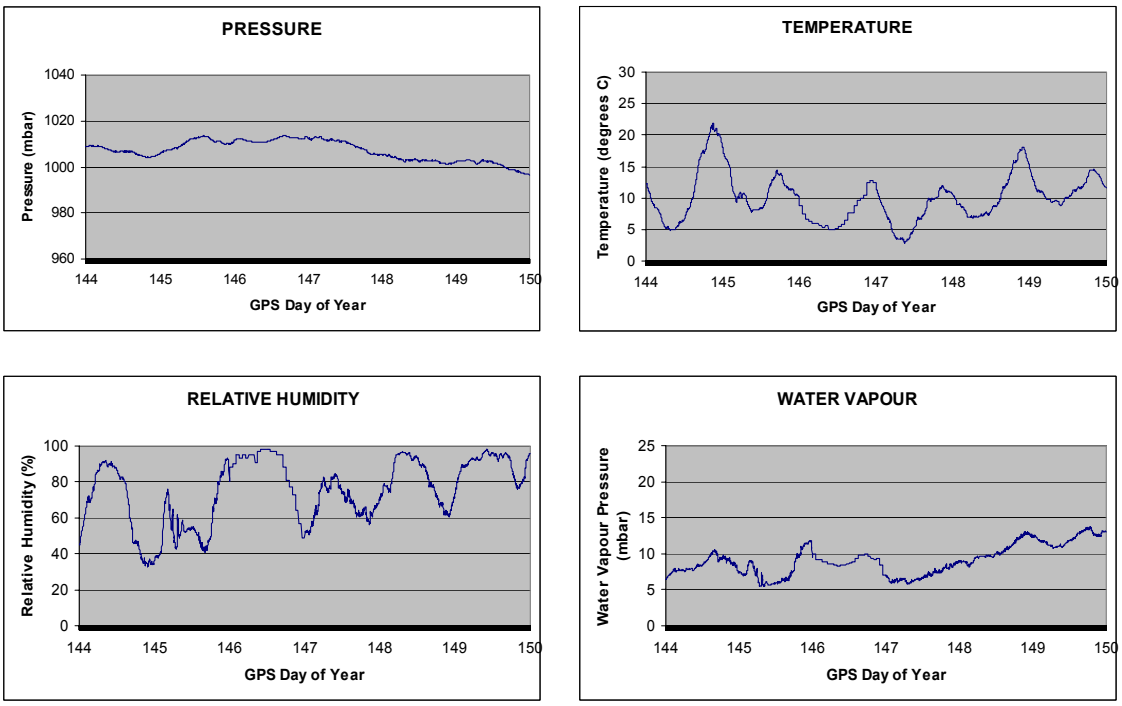

Figure E.2 Pressure, temperature, relative humidity, and water vapour pressure at GPS reference station UNB1 for days 144 to 149.

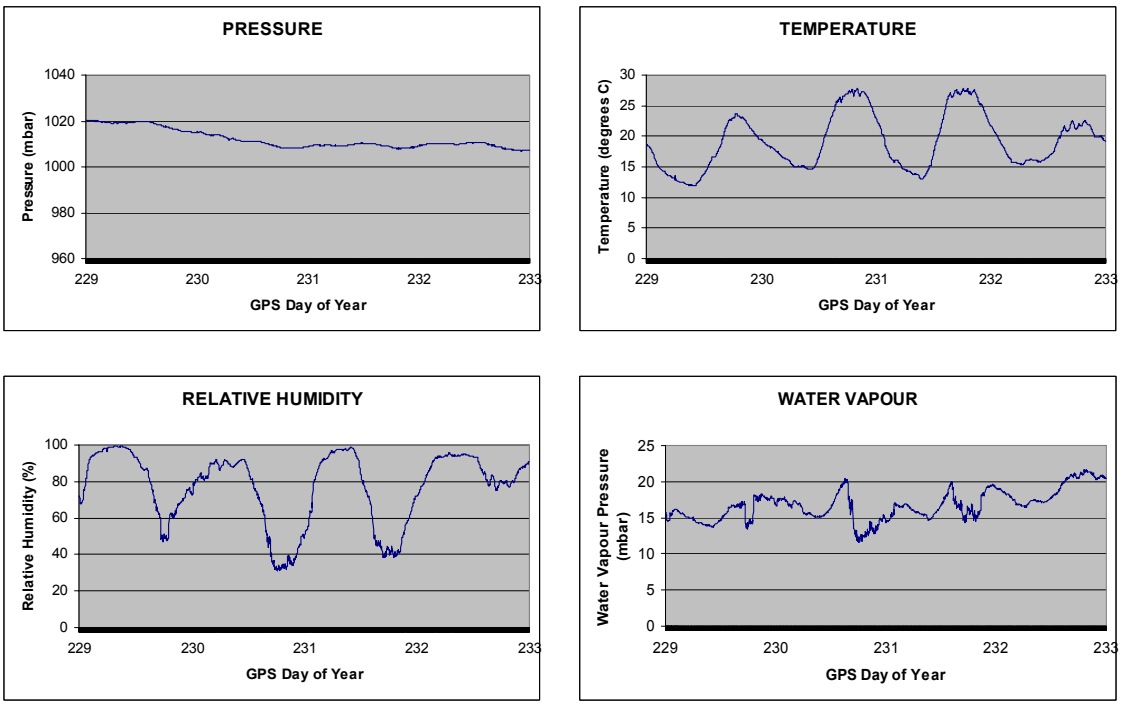

Figure E.3 Pressure, temperature, relative humidity, and water vapour pressure at GPS reference station UNB1 for days 229 to 232.

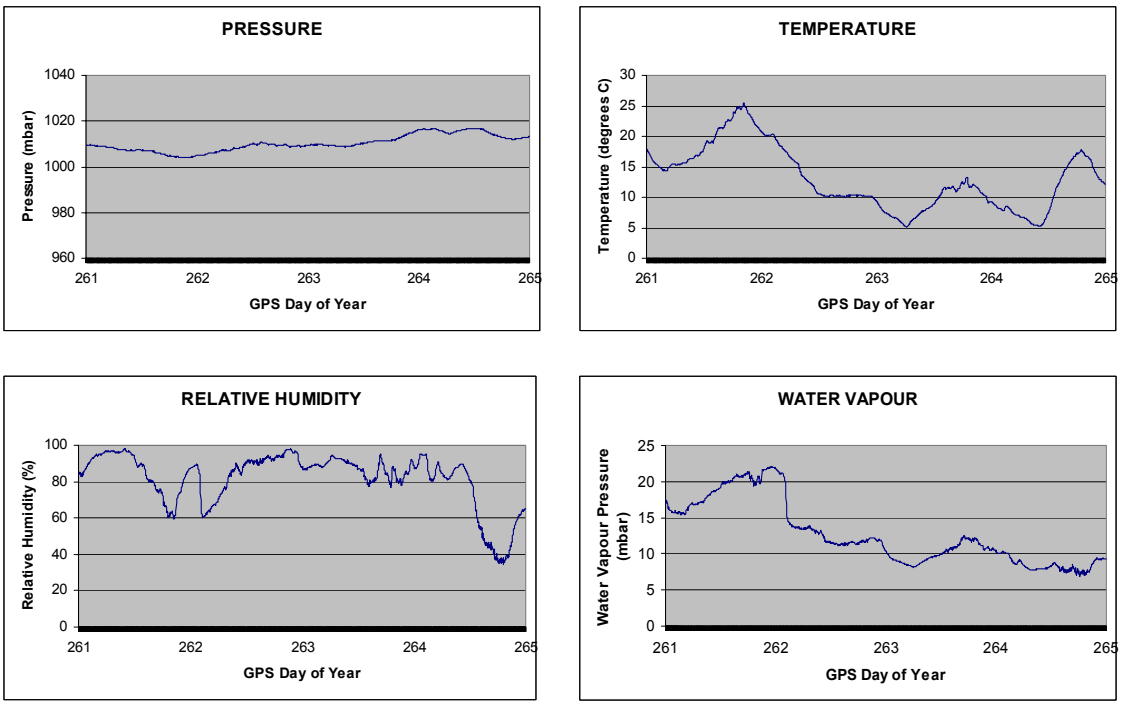

Figure E.4 Pressure, temperature, relative humidity, and water vapour pressure at GPS station UNB1 for days 261 to 264.

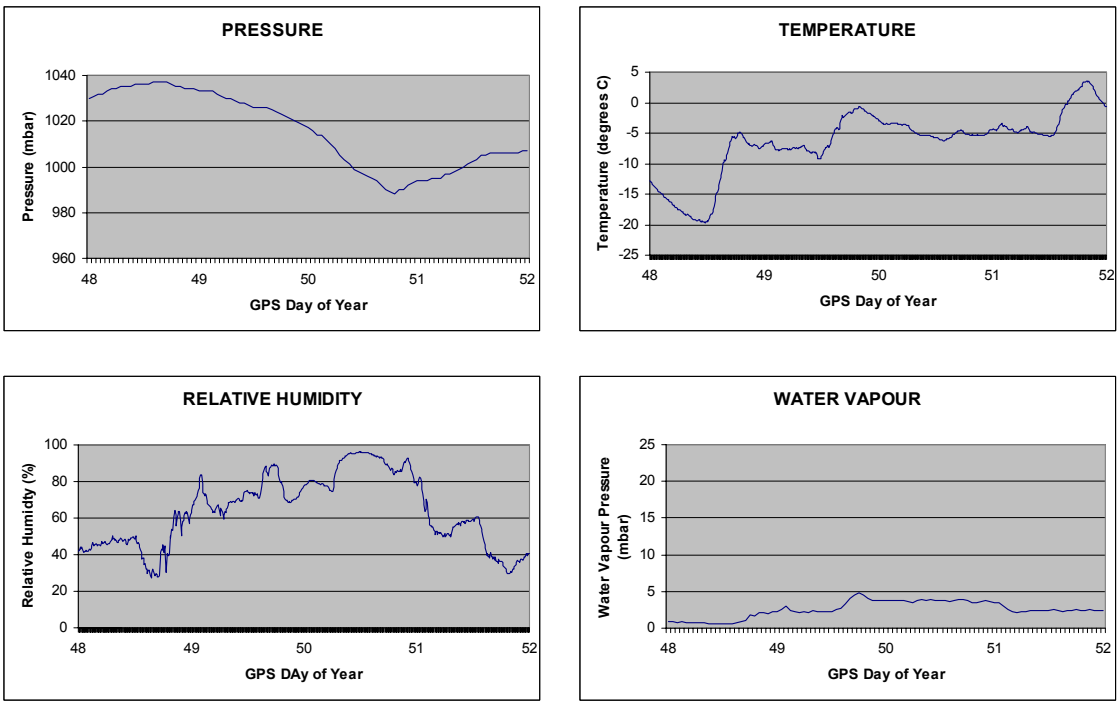

Figure E.5 Pressure, temperature, relative humidity, and water vapour pressure at GPS station CGSJ for days 48-51.

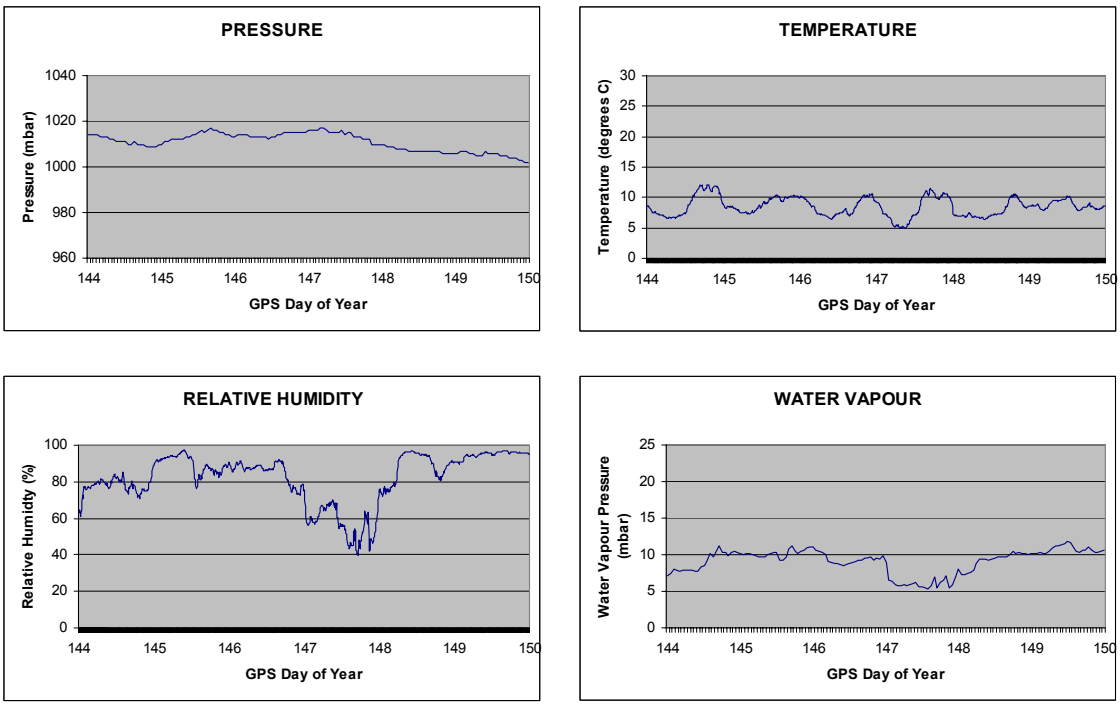

Figure E.6 Pressure, temperature, relative humidity, and water vapour pressure at GPS station CGSJ for days 144 to 149.

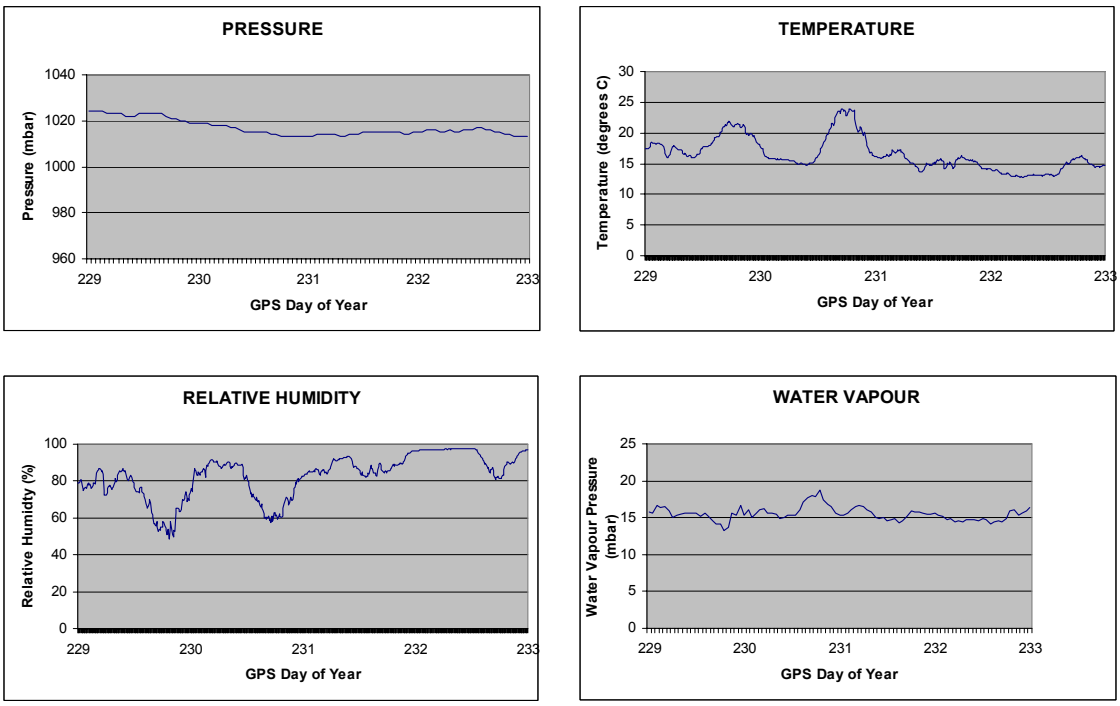

Figure E.7 Pressure, temperature, relative humidity, and water vapour pressure at GPS station CGSJ for days 229 to 232.

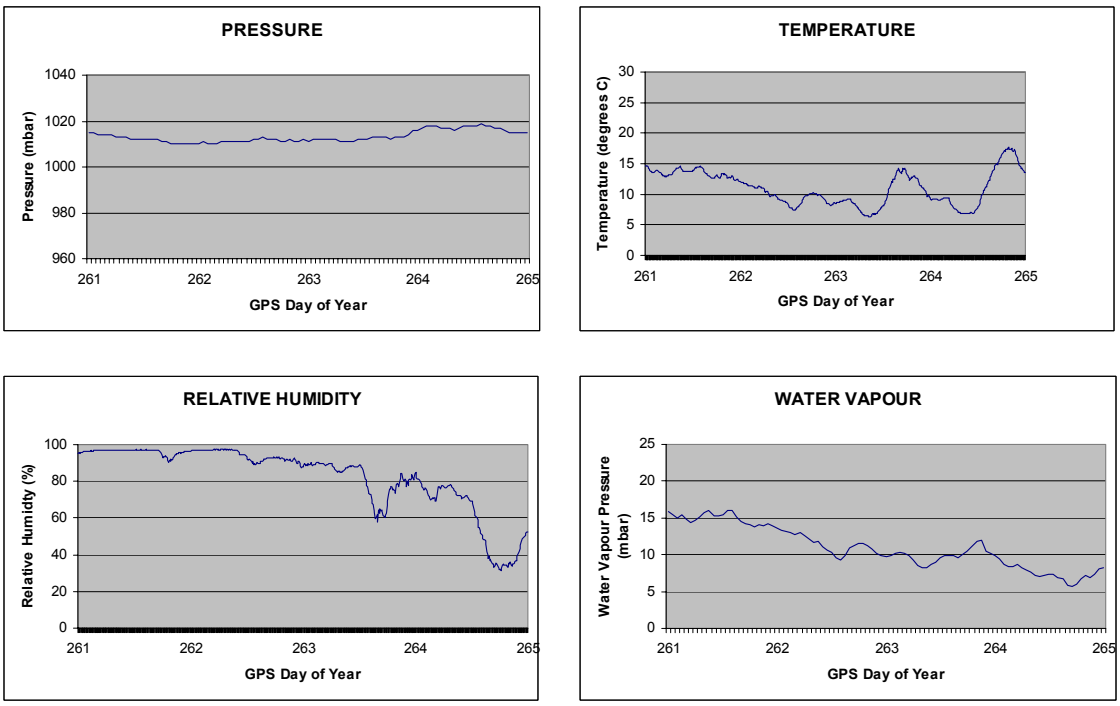

Figure E.8 Pressure, temperature, relative humidity, and water vapour pressure at GPS station CGSJ for days 261 to 264.

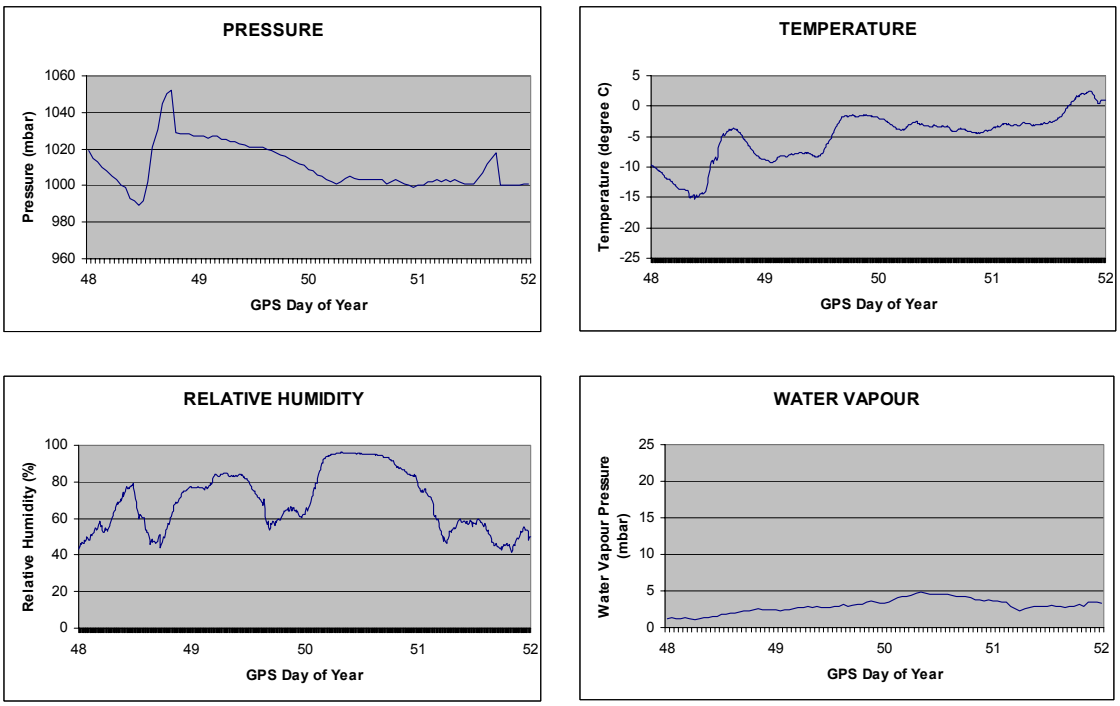

Figure E.9 Pressure, temperature, relative humidity, and water vapour pressure at GPS station DRHS for days 48 to 51.

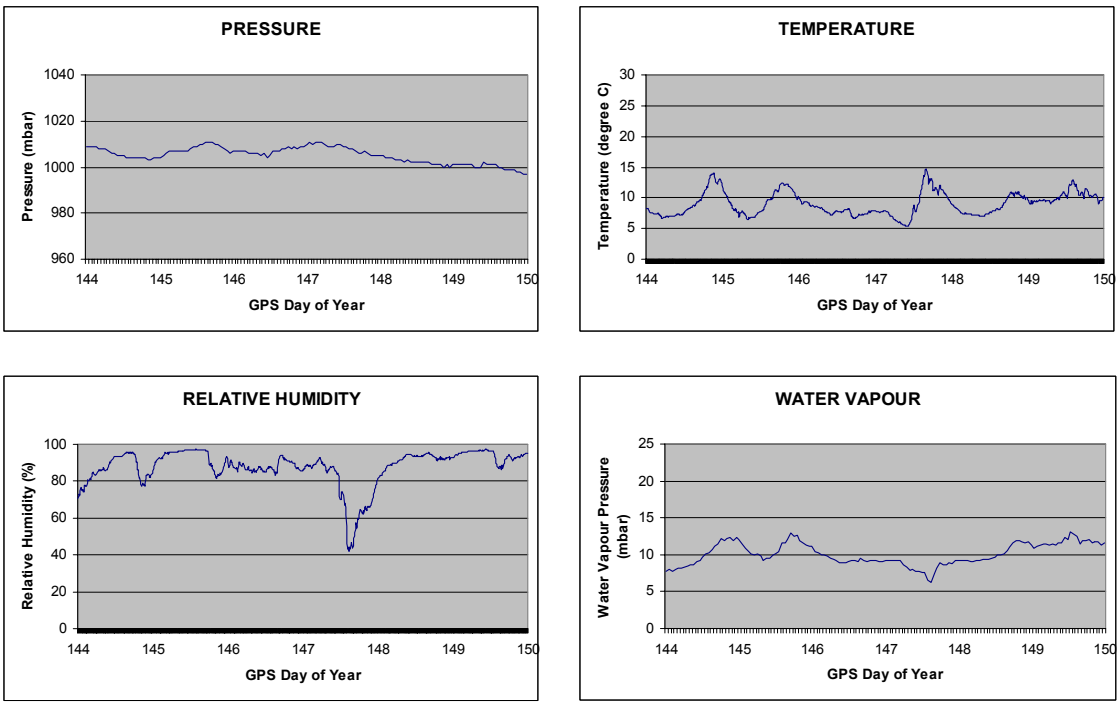

Figure E.10 Pressure, temperature, relative humidity, and water vapour pressure at GPS station DRHS for days 144 to 149.

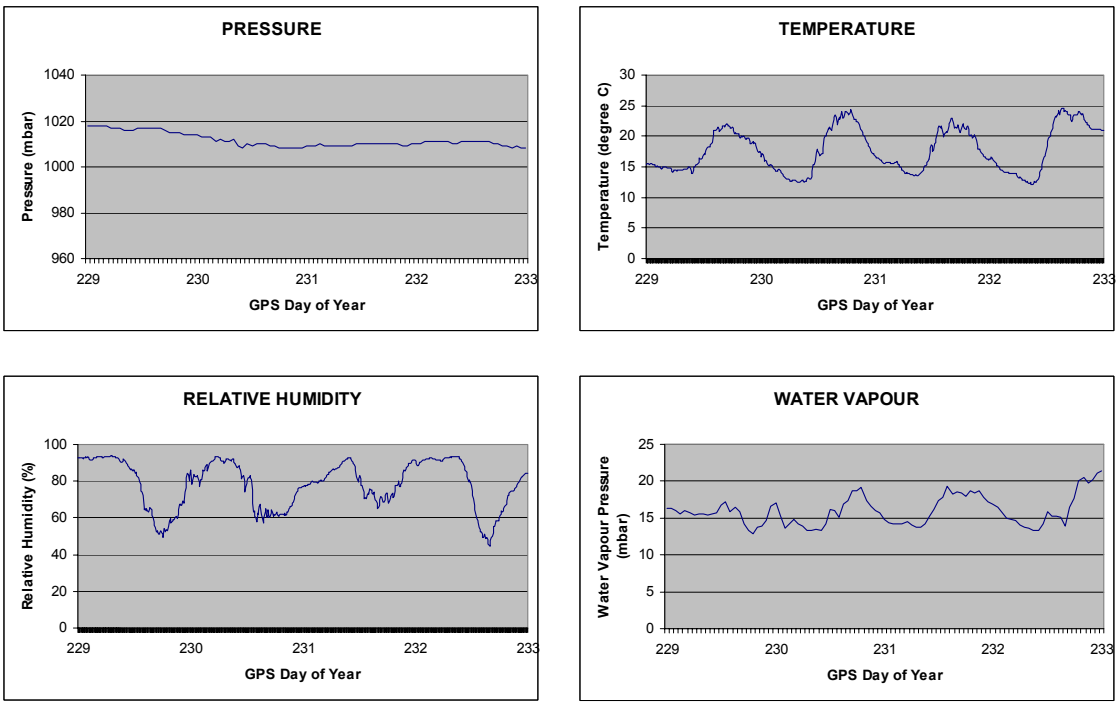

Figure E.11 Pressure, temperature, relative humidity, and water vapour pressure at GPS station DRHS for days 229 to 232.

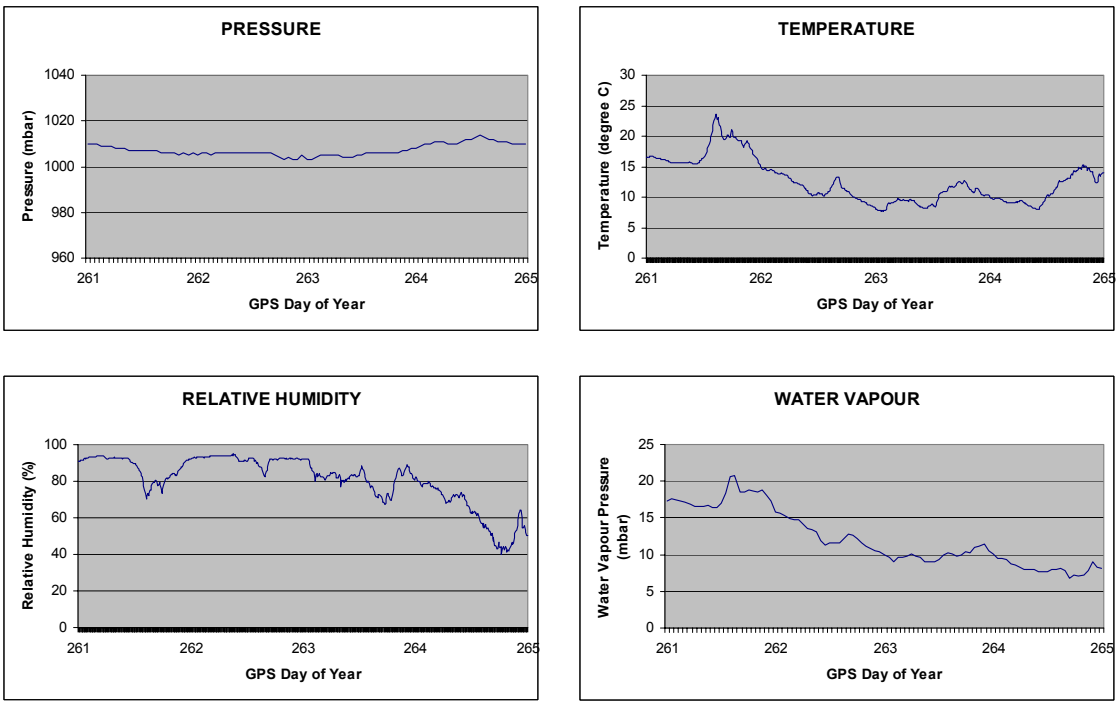

Figure E.12 Pressure, temperature, relative humidity, and water vapour pressure at GPS station DRHS for days 261 to 264.

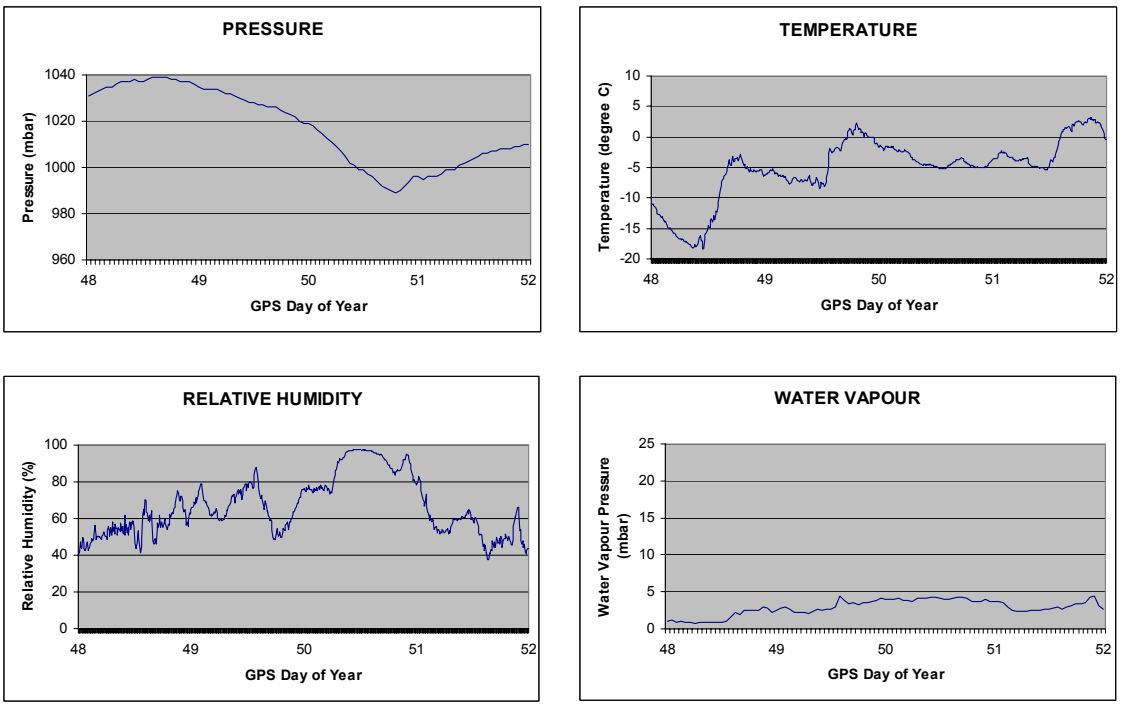

Figure E.13 Pressure, temperature, relative humidity, and water vapour pressure at GPS station BOAT for days 48 to 51.

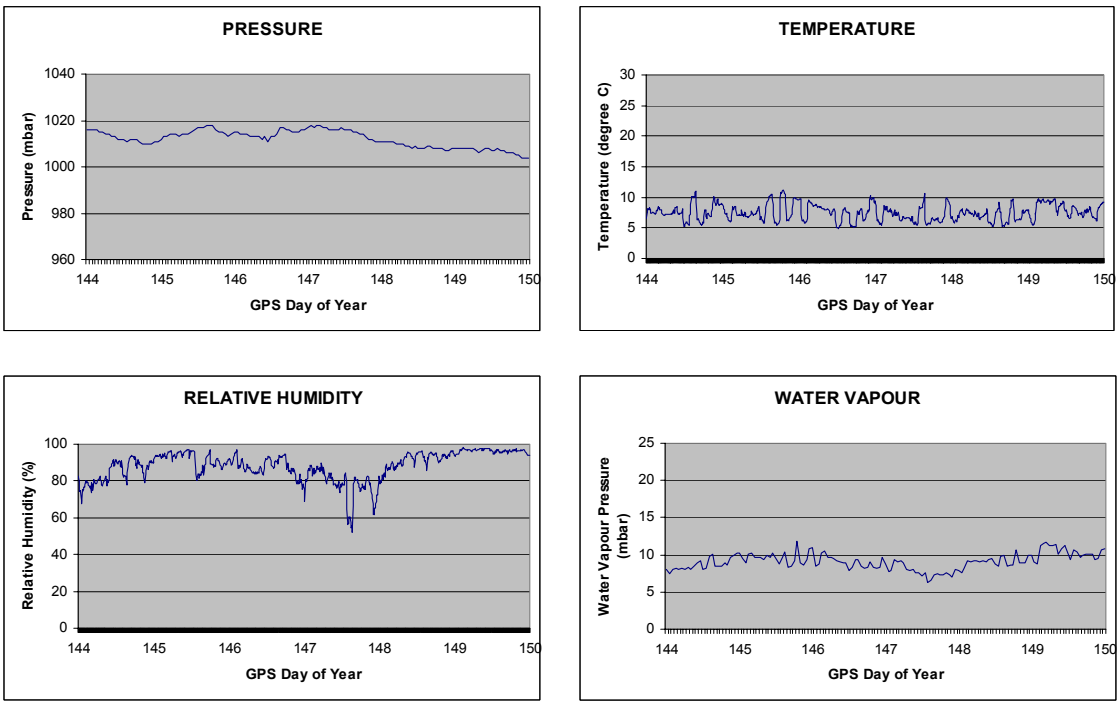

Figure E.14 Pressure, temperature, relative humidity, and water vapour pressure at GPS station BOAT for days 144 to 149.

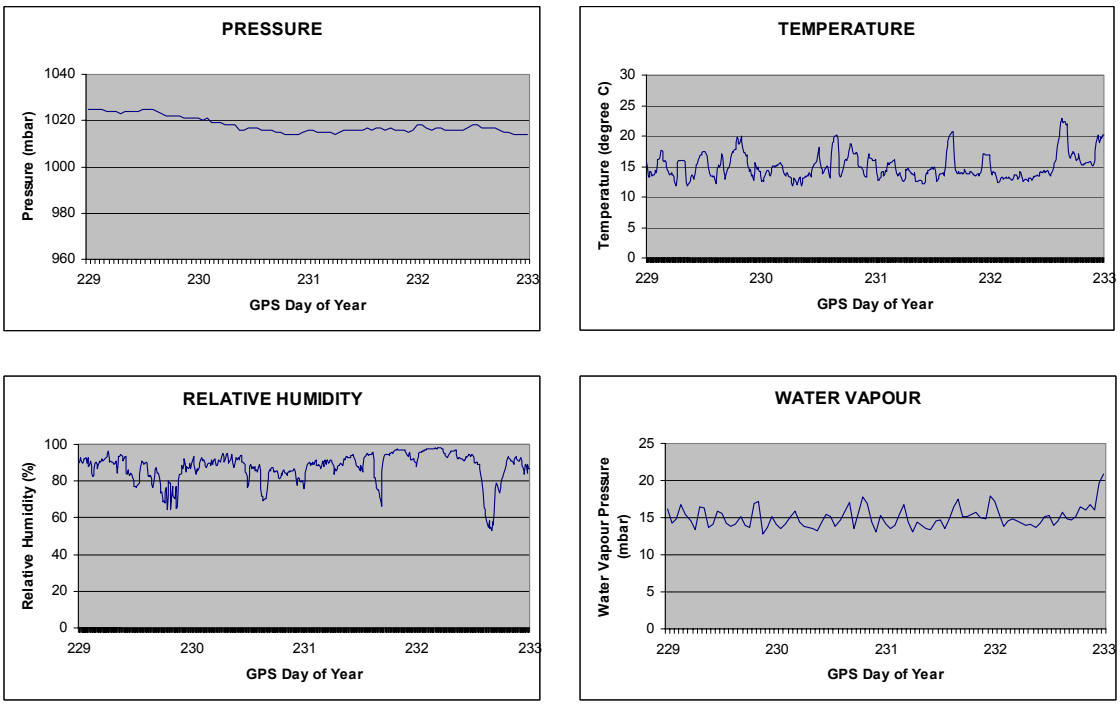

Figure E.15 Pressure, temperature, relative humidity, and water vapour pressure at GPS station BOAT for days 229 to 232.

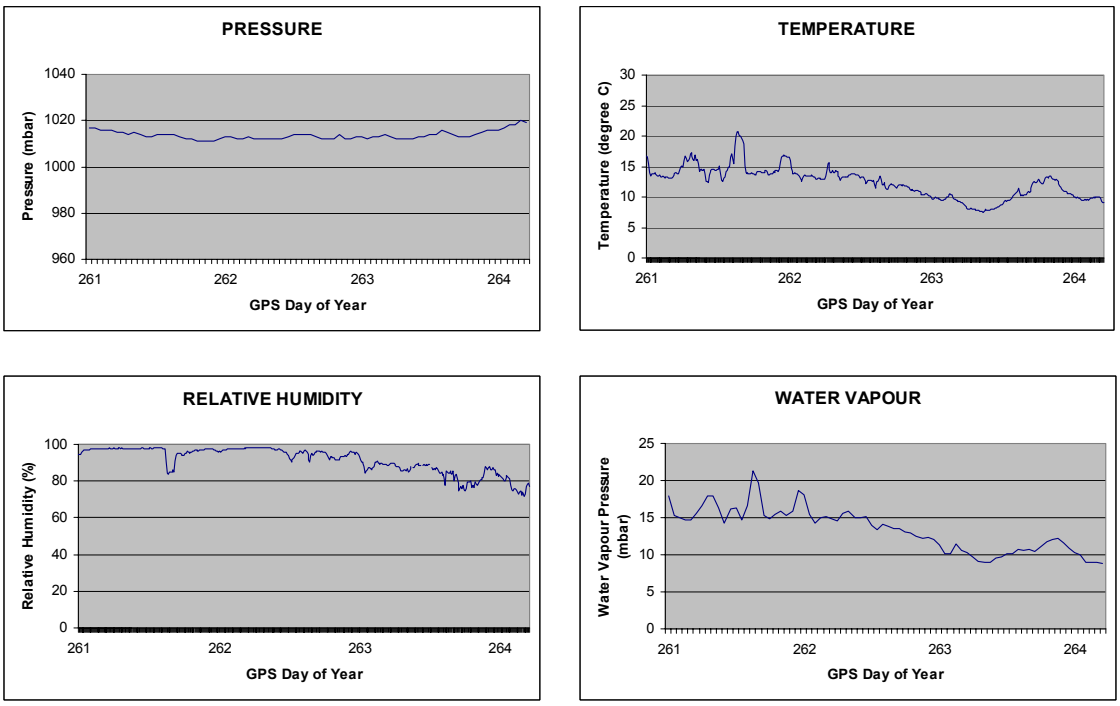

Figure E.16 Pressure, temperature, relative humidity, and water vapour pressure at GPS station BOAT for days 261 to 264.

APPENDIX F - Daily results for measurement domain tests

Table F.1 Standard deviation, mean and RMS (in millimetres) of differences in zenith delays for station UNB1. IGS minus model delays.

Day	RMS Error in Estimation of zenith tropospheric delay								
	IGS – NWP (in mm)			IGS – SAAS (in mm)			IGS – SAAS std (in mm)		
	St. Dev.	Mean	RMS	St. Dev.	Mean	RMS	St. Dev.	Mean	RMS
48	4.5	5.0	6.6	26.9	-22	34.6	18.5	-45.5	48.3
49	4.0	5.0	6.3	7.8	11.3	13.7	14.0	-65.6	67.0
50	7.6	14.4	16.2	17.5	25.0	30.3	10.5	-93.4	94.0
51	3.5	13.2	13.4	8.2	5.6	9.9	5.9	-120.7	118.4

Table F.2 Standard deviation, mean and RMS (in millimetres) of differences in zenith delays for station UNB1. IGS minus model delays.

Day	RMS Error in Estimation of zenith tropospheric delay (m)								
	IGS – NWP (in mm)			IGS – SAAS (in mm)			IGS – SAAS std (in mm)		
	St. Dev.	Mean	RMS	St. Dev.	Mean	RMS	St. Dev.	Mean	RMS
144	19.9	7.0	20.7	14.4	31.2	34.2	18.7	-15.3	23.9
145	13.3	2.9	13.3	30.5	40.7	50.5	39.3	-4.8	38.8
146	4.4	11.6	12.4	18.7	53.3	56.3	19.3	25.2	31.5
147	8.5	8.2	11.7	23.2	56.6	60.9	24.0	3.5	23.8
148	13.3	3.4	13.5	41.1	37.9	55.3	31.5	1.8	30.9
149	8.0	4.5	9.0	19.0	13.0	22.7	18.8	-9.0	20.5

Table F.3 Standard deviation, mean and RMS (in millimetres) of differences in zenith delays for station UNB1. IGS minus model delays.

Day	RMS Error in Estimation of zenith tropospheric delay								
	IGS – NWP (in mm)			IGS – SAAS (in mm)			IGS – SAAS std (in mm)		
	St. Dev.	Mean	RMS	St. Dev.	Mean	RMS	St. Dev.	Mean	RMS
229	26.2	4.3	26.1	13.0	4.5	13.5	13.2	54.5	56.0
230	11.8	3.7	12.1	23.8	7.7	24.6	32.4	41.9	52.5
231	11.2	17.8	21.0	16.7	-1.6	16.4	16.1	34.2	37.7
232	9.3	27.1	28.1	12.8	10.1	16.2	19.8	73.8	75.0

Table F.4 Standard deviation, mean and RMS (in millimetres) of differences in zenith delays for station UNB1. IGS minus model delays.

Day	RMS Error in Estimation of zenith tropospheric delay								
	IGS – NWP (in mm)			IGS – SAAS (in mm)			IGS – SAAS std (in mm)		
	St. Dev.	Mean	RMS	St. Dev.	Mean	RMS	St. Dev.	Mean	RMS
261	23.0	7.0	23.6	32.7	6.9	32.8	24.1	60.6	65.0
262	24.4	25.5	34.9	33.9	67.0	74.8	14.3	72.4	73.7
263	9.4	6.9	11.5	12.7	-10.2	16.1	17.4	-29.0	33.6
264	4.5	5.0	6.6	26.9	-22.2	34.6	18.5	-45.5	48.3

APPENDIX G - Zenith total delays at station CGSJ

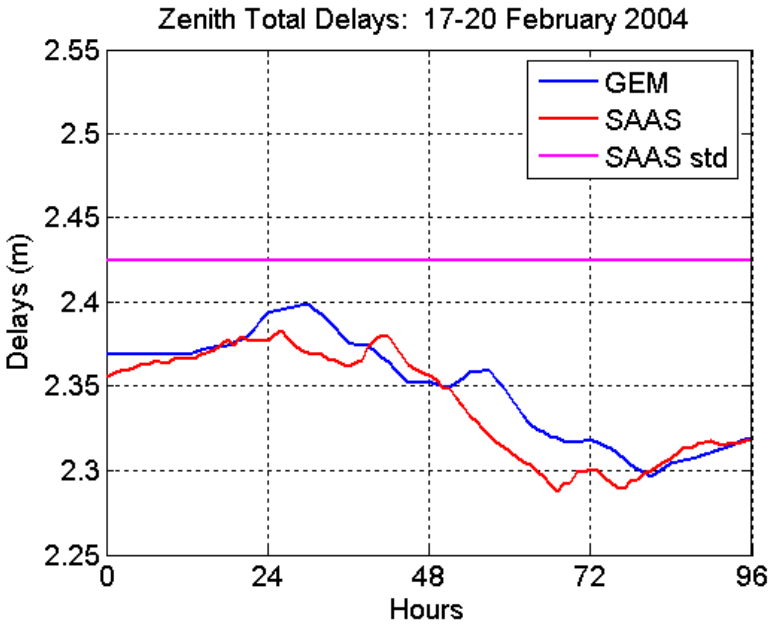

Figure G.1 Zenith total delay values determined for days 48 to 51 at GPS station CGSJ.

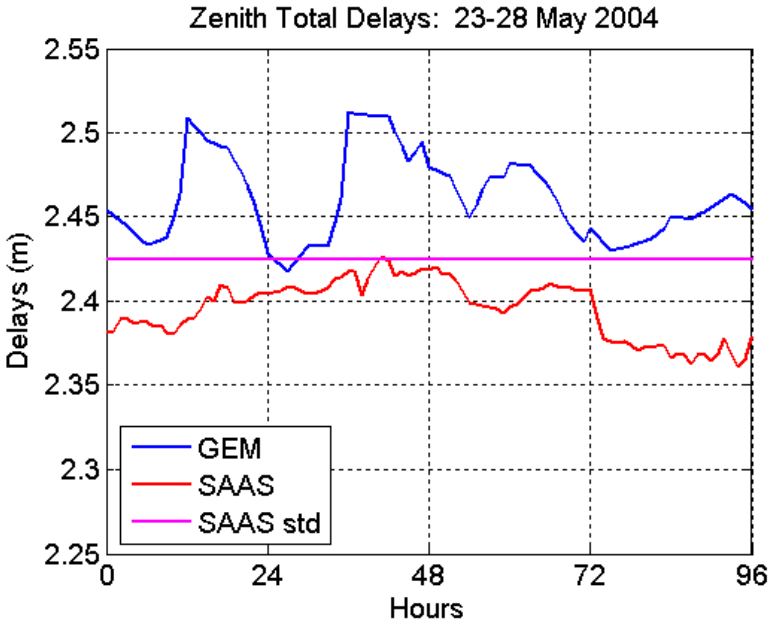

Figure G.2 Zenith total delay values determined for days 144 to 149 at GPS station CGSJ.

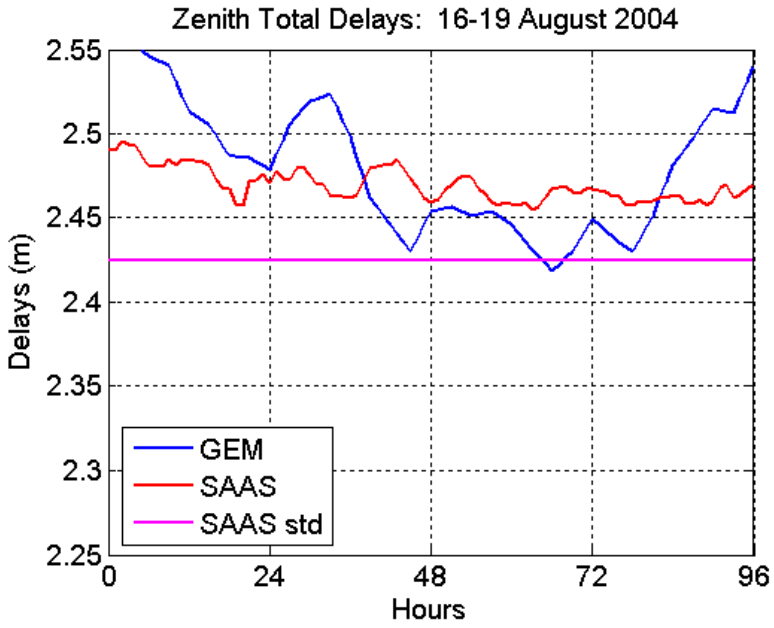

Figure G.3 Zenith total delay values determined for days 229 to 232 at GPS station CGSJ.

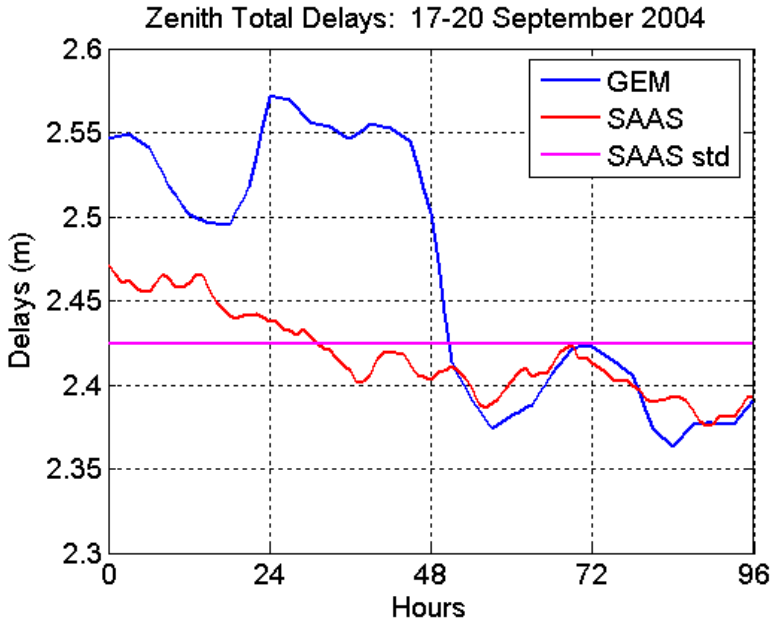

Figure G.4 Zenith total delay values determined for days 261 to 264 at GPS station CGSJ.

APPENDIX H – Histogram plots of differences in total zenith delay.

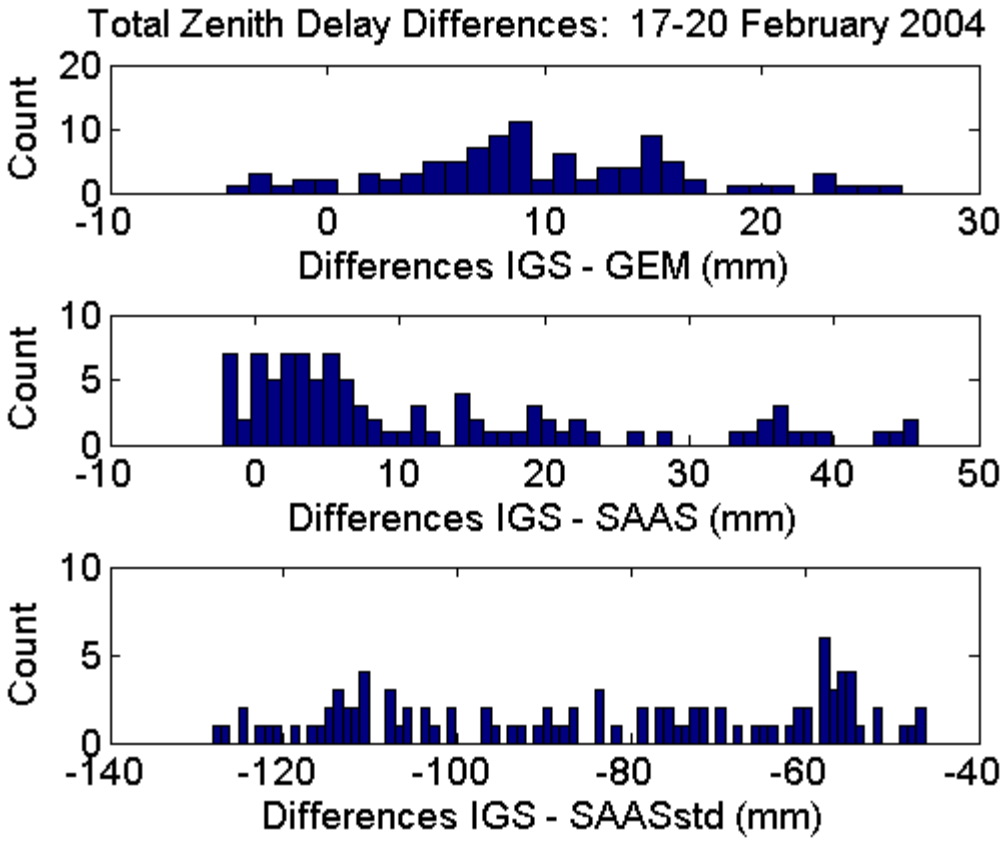

Figure H.1 Histogram of differences in total zenith delay for days 48 to 51 at GPS station UNB1.

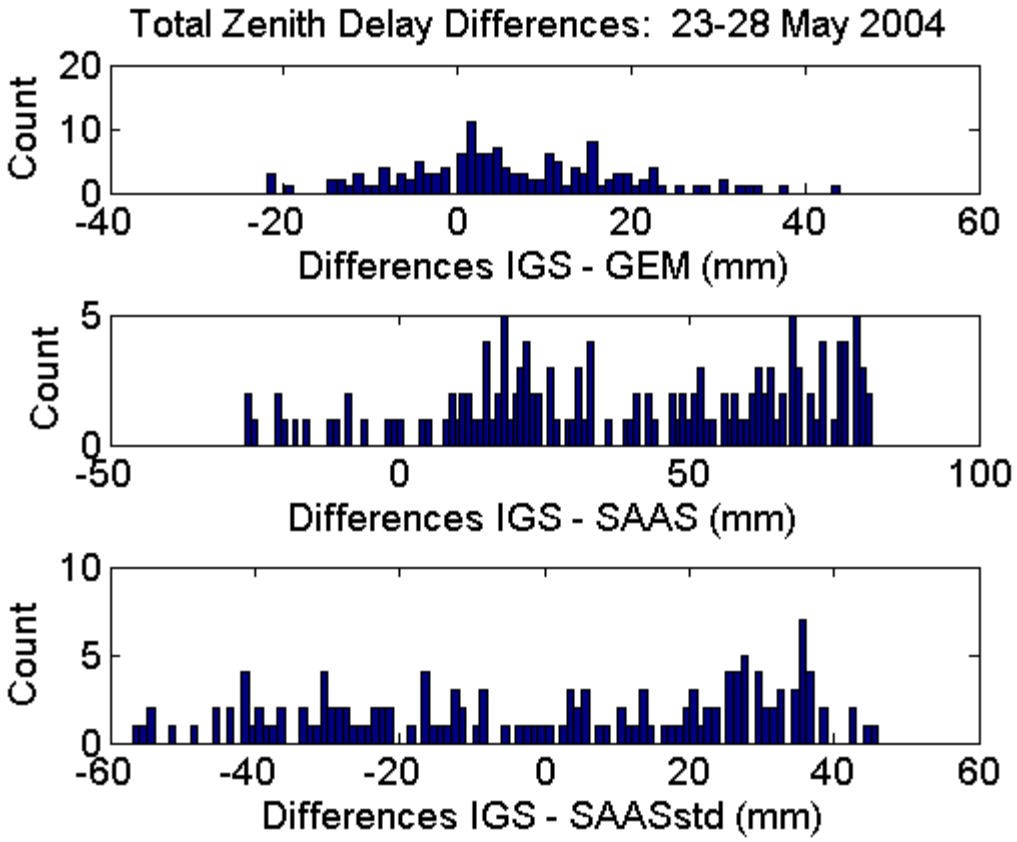

Figure H.2 Histogram of differences in total zenith delay for days 144 to 149 at GPS station UNB1.

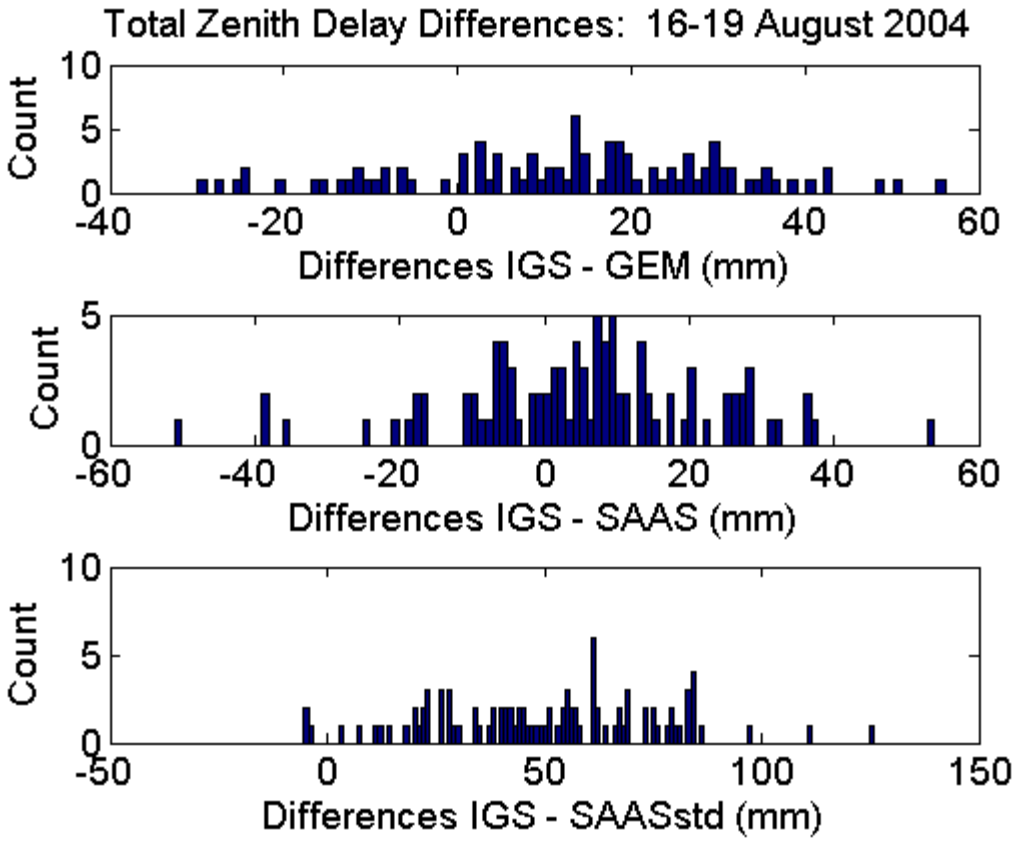

Figure H.3 Histogram of differences in total zenith delay for days 229 to 232 at GPS station UNB1.

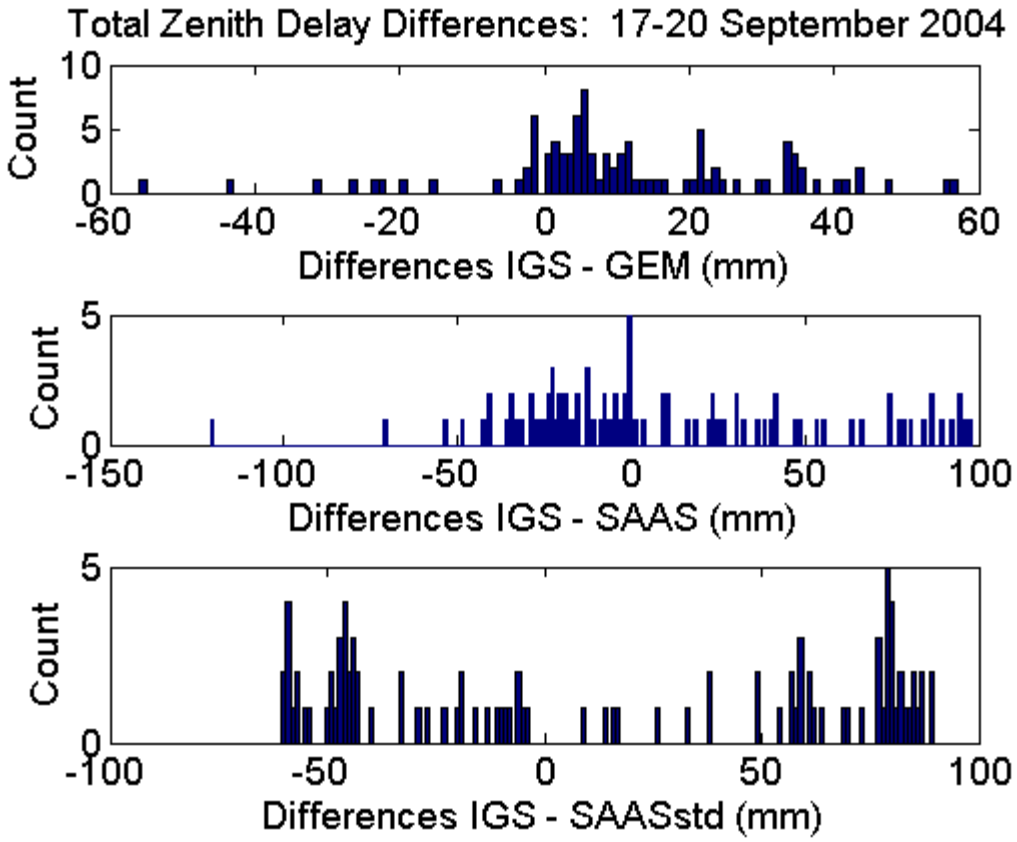

Figure H.4 Histogram of differences in total zenith delay for days 262 to 264 at GPS station UNB1.

Name: Karen Maureen Cove

Address: 667 Reid Street
Fredericton
New Brunswick
Canada E3B 3V6

Born: April 29, 1973
Halifax, Nova Scotia, Canada

School: University of New Brunswick, Fredericton, New Brunswick
Degree: Bachelor of Science in Engineering, 2002

List of Publications:

Cove, K., and M. Santos (2004). "An analysis of carrier-phase differential positioning using Dynapos." *GPS Solutions*, Vol. 8, No. 4, pp. 210-216.

Cove, K., M. Santos, D. Wells, and S. Bisnath (2004). "Improved Tropospheric Delay Estimation for Long Baseline, Carrier-Phase Differential GPS Positioning in a Coastal Environment." In proceedings on Institute of Navigation GNSS 2004, Long Beach, California, USA, 21-24 September 2004.

Santos, M., D. Wells, **K. Cove**, and S. Bisnath (2004). " The Princess of Acadia GPS Project: Description and Scientific Challenges." In proceedings on Canadian Hydrographic Conference 2004, Ottawa, Ontario, Canada, 24-27 May 2004.

Bisnath, S., D. Wells, M. Santos, and **K. Cove** (2004). "Initial Results from a Long Baseline, Kinematic, Differential GPS Carrier Phase Experiment in a Marine Environment." In proceedings on PLANS 2004, Monteray, California, 26-29 April 2004.

Cove, K., M. Santos, L. Huff, B. Remondi, and D. Wells (2003). "Assessment of Performance of Ionospheric Delay-Free GPS Carrier Phase Kinematic Relative Positioning With Varying Baseline Lengths." In proceedings on Hydro US 2003, Biloxi, Mississippi, USA, 24-27 March 2003.

Cove, K. (2002). "Property Rights Regime for Offshore oil and Gas Development." Unpublished technical report in the Department of Geodesy and Geomatics Engineering, University of New Brunswick, Fredericton, New Brunswick, Canada.

List of Conference Presentations:

Cove, K. (2004). "Princess of Acadia GPS Project. " Poster presented at Geomatics Atlantic Conference, Fredericton, New Brunswick, Canada, 7-9 June 2004.

Santos, M., M. Al-Shari, **K. Cove**, C. Solomon, D. Wells, and S. Bisnath (2004)."Goals and Early results of the Princess of Acadia GPS Project." American Geophyical Union 2004 Joint Assembly, Montreal, Canada, 17-21 May 2004.

Wells, D., S. Bisnath, S. Howden, D. Dodd, M. Santos, **K. Cove**, D. Kim, and B. Remondi (2004). "Prospects for Extended-Range Marine PPK." International Navigation Conference MELAHA 2004, Cairo, Egypt, 13-15 April 2004.

Cove, K. and M. Santos (2004). "Initial Results and Future Goals for the Princess of Acadia Project." Presentation for Real-Time Kinematic GPS Navigation for Hydrography Surveys and Seamless Vertical Datums Workshop, Long Beach, Mississippi, USA, 16-18 March 2004.

Cove, K. and M. Santos (2002). "Carrier Phase Differential Kinematic GPS Data Processing and Analysis." Presentation for Real-Time Kinematic GPS Navigation for Hydrography Surveys and Seamless Vertical Datums Workshop, Stennis Space Center, Mississippi, USA, 26-28 August.